



**Document Number: H2020-ICT-52/RISE-6G/D5.3**

Project Name:

**Reconfigurable Intelligent Sustainable Environments for 6G Wireless Networks  
(RISE-6G)**

## **Deliverable D5.3**

# **Control for RIS-based localisation and sensing (Final Specifications)**

Date of delivery: 30/06/2023

Version: 1.0

Start date of Project: 01/01/2021

Duration: 36 months



### Deliverable D5.3

#### Control for RIS-based localisation and sensing (Final Specifications)

Project Number:	101017011
Project Name:	<b>Reconfigurable Intelligent Sustainable Environments for 6G Wireless Networks</b>

<b>Document Number:</b>	H2020-EUK-815323/RISE-6G/D5.3
<b>Document Title:</b>	Control for RIS-based localisation and sensing (Final Specifications)
<b>Editor(s):</b>	Benoît Denis (CEA)
<b>Authors:</b>	Henk Wymeersch (CHAL), Hyowon Kim (CHAL), George Alexandropoulos (NKUA), Benoit Denis (CEA), Petar Popovski (AAU), Vincenzo Sciancalepore (NEC), Radoslaw Kotaba (AAU), Kimmo Kansanen (AAU), Fabio Saggese (AAU), Musa Furkan Keskin (CHAL), Hyowon Kim (CHAL), Moustafa Rahal (CEA), Antonio Albanese (NEC), Placido Mursia (NEC), Paolo Di Lorenzo (CNIT), Francesca Costanzo (CNIT), Kyriakos Stylianopoulos (NKUA).
<b>Dissemination Level:</b>	PU
<b>Contractual Date of Delivery:</b>	30/06/2023
<b>Security:</b>	Public
<b>Status:</b>	Final
<b>Version:</b>	1.0
<b>File Name:</b>	RISE-6G_WP5_D5.3_V1.0.docx



## Abstract

This deliverable provides the final proposals of RISE-6G regarding physical architectures, control schemes, signalling, and data flows, in relation to work package 5 “RIS for Enhanced Localisation and Sensing”, as well as a description of a few candidate solutions selected for future validations through lab demonstrations and field trials. It is also and foremost meant to serve as a basis for the definition of the final RISE-6G architecture, specifying key logical blocks and their interfaces.

## Keywords

Beyond-5G; 6G; RIS; Localisation; Sensing; Control; Architecture.





## Table of Contents

<b>1</b>	<b>Introduction .....</b>	<b>15</b>
1.1	Deliverable objectives .....	15
1.2	Deliverable structure .....	15
1.3	Disclaimer on RISE-6G architecture definition with respect to project timeline. ....	16
<b>2</b>	<b>Localisation and sensing basics .....</b>	<b>16</b>
2.1	Foundations of localisation.....	16
2.2	From localisation to sensing.....	17
2.3	RIS-aided localisation and sensing .....	18
2.4	Key performance indicators and their evaluation .....	19
2.4.1	Localisation and sensing performance metrics.....	19
2.4.2	Methods and evaluation.....	19
<b>3</b>	<b>Motivations for new architectures and control schemes in RIS-aided localisation and sensing</b>	<b>19</b>
3.1	Architectures for RIS-aided localisation and sensing.....	19
3.1.1	General RISE-6G architecture proposal .....	20
3.1.2	Specific requirements and challenges in RIS-aided localisation and sensing .....	20
3.2	Control schemes for RIS-aided localisation and sensing.....	22
3.3	Signalling and protocols for RIS-aided localisation and sensing.....	24
3.3.1	RIS signalling.....	24
3.3.2	RIS protocols.....	24
<b>4</b>	<b>RISE-6G architecture and control proposals for RIS-aided localisation and sensing .....</b>	<b>24</b>
4.1	Summary of RISE-6G proposals .....	25
4.2	Single-BS UE localisation with reflective RISs (C1) .....	26
4.2.1	Context and motivations.....	26
4.2.2	Overall system description .....	26
4.2.3	Results .....	29
4.2.4	Perspectives .....	29
4.3	Passive RIS localisation with several BSs (C2).....	30
4.3.1	Context and motivations.....	30
4.3.2	Overall system description .....	30
4.3.3	Results .....	32
4.3.4	Perspectives .....	33
4.4	BS-free UE localisation and environment mapping with one reflective RIS (C3) .....	33
4.4.1	Context and motivations.....	33



4.4.2	Overall system description .....	33
4.4.3	Results .....	35
4.4.4	Perspectives .....	36
<b>4.5</b>	<b>BS-free cooperative UE localisation through sidelinks with one reflective RIS (C4) ....</b>	<b>37</b>
4.5.1	Context and motivations .....	37
4.5.2	Overall system description .....	37
4.5.3	Results .....	38
4.5.4	Perspectives .....	39
<b>4.6</b>	<b>Single-BS UE localisation with one reflective RIS in near field (C5) .....</b>	<b>39</b>
4.6.1	Context and motivations .....	39
4.6.2	Overall system description .....	39
4.6.3	Results .....	42
4.6.4	Perspectives .....	44
<b>4.7</b>	<b>Single-BS UE localisation with one reflective RIS in near field under real hardware constraints (C6) .....</b>	<b>44</b>
4.7.1	Context and motivations .....	44
4.7.2	Overall system description .....	45
4.7.3	Results .....	46
4.7.4	Perspectives .....	48
<b>4.8</b>	<b>BS-free UE localisation with several sensing RISs (C7) .....</b>	<b>48</b>
4.8.1	Context and motivations .....	48
4.8.2	Overall system description .....	49
4.8.3	Results .....	50
4.8.4	Perspectives .....	51
<b>4.9</b>	<b>BS-free UE localisation with one partially-connected sensing RIS (C8) .....</b>	<b>51</b>
4.9.1	Context and motivations .....	51
4.9.2	Overall system description .....	51
4.9.3	Results .....	52
4.9.4	Perspectives .....	53
<b>4.10</b>	<b>Single-BS NLoS UE localisation with several reflective RISs (C9) .....</b>	<b>53</b>
4.10.1	Context and motivations .....	53
4.10.2	Overall system description .....	53
4.10.3	Results .....	55
4.10.4	Perspectives .....	56
<b>4.11</b>	<b>Localisation of both active and passive UEs with one sensing RIS (C10) .....</b>	<b>57</b>
4.11.1	Context and motivations .....	57
4.11.2	Overall system description .....	57
4.11.3	Results .....	59



---

Document:	H2020-ICT-52/RISE-6G/D5.3		
Date:	30/06/2023	Security:	Public
Status:		Version:	1.0

---

4.11.4	Perspectives .....	60
<b>5</b>	<b>Candidate architectures and control schemes for physical laboratory demonstrations and field trials of RIS-aided localisation and sensing .....</b>	<b>60</b>
<b>5.1</b>	<b>Offline laboratory experiments.....</b>	<b>60</b>
5.1.1	Experimental validation of single-BS localization and mapping at 28 GHz .....	60
5.1.2	Experimental validation of RIS-aided self-localization at 60 GHz .....	63
5.1.3	RIS-aided fingerprinting positioning at 3.7 GHz .....	65
<b>5.2</b>	<b>Online field trials.....</b>	<b>66</b>
5.2.1	RIS-aided Single-BS localization with commercial network and equipment in a factory environment at 27 GHz.....	66
<b>6</b>	<b>Conclusions and final recommendations .....</b>	<b>67</b>
<b>7</b>	<b>References.....</b>	<b>70</b>



Document:	H2020-ICT-52/RISE-6G/D5.3		
Date:	30/06/2023	Security:	Public
Status:		Version:	1.0

## List of Figures

Figure 2-1: Example of RTT-based localisation (left), constraining the UE on the intersection of circles (2D) or spheres (3D); localisation based on DL-AoD measurements (middle), constraining the user within a sector of each BS; localisation based on near-field measurements exploiting the wavefront curvature (right).....	17
Figure 2-2: Different form of sensing. ....	18
Figure 2-3: Examples of use of RIS in localisation: a new signal path via a RIS and a new reference by the RIS (left); large RIS provides wavefront curvature for localisation measurements (middle); a RIS provides a signal path to avoid signal blockage in monostatic sensing [RIS5.2-22]. ....	18
Figure 3-1: Localisation and sensing time scales. ....	22
Figure 4-1: C1 - Physical deployment vs. architecture requirements, in terms of control signalling and data (* means that data is transmitted on the over-the-air interface).....	27
Figure 4-2: C1 - Messages sequence chart. ....	28
Figure 4-3: C1 - Time diagram.....	29
Figure 4-4: CDF of estimation error and CRLB bounds of directional and random RIS phase profiles for a) UE position, b) UE clock bias, and c) UE velocity. The UE has the position $[-10, 10, -10]$ with the velocity $[-v, v, 0]$ , where $v$ is between 0 and 30 m/s.....	29
Figure 4-5: C2 - Physical deployment vs. architecture requirements, in terms of control signalling and data (* means that data is transmitted on the over-the-air interface).....	31
Figure 4-6: C2 - Messages sequence chart. ....	31
Figure 4-7: C2 - Time diagram.....	32
Figure 4-8: Performance of passive RIS localisation: (a) PEB of the RIS position in meters for three RXs (shown by red triangles) and one Tx (marked by black star); and (b) CDF of PEB (solid lines) and estimation error for 100 random RIS configurations.....	32
Figure 4-9: RMSEs and error bounds of the RIS position and orientation as a function of the transmission power, under the deployment of one Tx, one Rx, and one RIS.....	33
Figure 4-10: C3 - Physical deployment vs. architecture requirements, in terms of control signalling and data (* means that data is transmitted on the over-the-air interface).....	33
Figure 4-11: C3 - RIS phase profile for multiple spatially-uniform beams. ....	34
Figure 4-12: C3 - Messages sequence chart. ....	35
Figure 4-13: C3 - Time diagram.....	35
Figure 4-14: Beam patterns of the 2D RIS in the azimuth (a)-(c) and elevation (d)-(f) domains: (a) and (d) with directional phases; (b) and (e) with optimised phases; (c) and (f) with the proposed uniform phases. ....	36
Figure 4-15: Localisation performance over time steps: Mean Absolute Errors (MAEs) of (a) position and (b) heading estimates.....	36
Figure 4-16: Mapping performance over time steps: (a) reflection point and (b) scattering point. ....	36
Figure 4-17: C4 - Physical deployment vs. architecture requirements, in terms of control signalling and data (* means that data is transmitted on the over-the-air interface).....	37
Figure 4-18: C4 - Messages sequence chart. ....	38





Document:	H2020-ICT-52/RISE-6G/D5.3		
Date:	30/06/2023	Security:	Public
Status:		Version:	1.0

Figure 4-19: C4 - Time diagram.....	38
Figure 4-20: PEBs of RIS-enabled cooperative UE localisation for different sizes of RIS (in terms of the number of elements).....	39
Figure 4-21: Canonical scenario considering optimising reflective RIS profiles in NLOS SISO DL positioning.....	40
Figure 4-22: C5 - Physical deployment vs. architecture requirements, in terms of control signalling and data (* means that data is transmitted on the over-the-air interface).....	40
Figure 4-23: Illustration of orthonormalized beams, i.e., the steering beam (red), and its three derivatives w.r.t. spherical coordinates (respectively in blue, green, and orange), suitable to RIS-aided NF NLoS localisation. ....	41
Figure 4-24: C5 - Messages sequence chart. ....	41
Figure 4-25: C5- Time diagram.....	42
Figure 4-26: PEB heatmap (in dB), as a function of UE location ( $z = 0$ ) for a generic RIS response model (supporting NF), with one planar reflective RIS of $32 \times 32$ elements in $[0, 0, 0]$ m, one BS in $[5, 5, 0]$ m and a finite obstacle parallel to the y axis (black). ....	42
Figure 4-27: PEB comparison as a function for the UE-RIS distance, with the proposed optimised RIS profile, conventional directional and random codebook designs, for different numbers of transmissions T and different prior UE position uncertainty (for the directional design only). ....	43
Figure 4-28: PEB as a function of the UE-RIS distance for different variants of the problem solver (incl. the “unconstrained”, “optimise then constrain” and “constrain then optimise” schemes regarding RIS beams generation).....	43
Figure 4-29: Distribution of RIS element-wise complex reflection coefficients in the complex plane, according to the lookup tables of 3 real R-RIS prototypes designed in RISE-6G. ....	44
Figure 4-30: C6 - Physical deployment vs. architecture requirements, in terms of control signalling and data. ....	45
Figure 4-31: C6 - Messages sequence chart. ....	46
Figure 4-32: C6 - Time diagram.....	46
Figure 4-33: Examples of steering beam gains (unconstrained and approximated under RIS hardware constraints) in 1D, as a function of the azimuth angles, while accounting for the RIS element responses of real hardware prototypes through look-up tables. ....	47
Figure 4-34: Examples of steering beam gains (unconstrained and approximated under RIS hardware constraints) in 2D, as a function of both azimuth and elevation angles, while accounting for the RIS element responses of real hardware prototypes through look-up tables. ....	47
Figure 4-35: PEB as a function of RIS-UE distance for ideal and generated localisation-optimal RIS beams, as constrained by the real look-up tables of various characterized hardware prototypes.....	48
Figure 4-36: PEB as a function of RIS-UE azimuth angle for ideal and generated localisation-optimal RIS beams, as constrained by the real look-up tables of various characterized hardware prototypes.....	48
Figure 4-37: C7 - Physical deployment vs. architecture requirements, in terms of control signalling and data (* means that data is transmitted on the over-the-air interface).....	49
Figure 4-38: C7 - Messages sequence chart. ....	50
Figure 4-39: C7 - Time diagram.....	50



Document:	H2020-ICT-52/RISE-6G/D5.3		
Date:	30/06/2023	Security:	Public
Status:		Version:	1.0

Figure 4-40: C8 - Physical deployment vs. architecture requirements, in terms of control signalling and data. ....	51
Figure 4-41 C8 - Messages sequence chart. ....	52
Figure 4-42: C8 - Time diagram.....	52
Figure 4-43: RMSE as a function of transmit power, for the architecture proposal of C8.....	53
Figure 4-44: C9 - Physical deployment vs. architecture requirements, in terms of control signalling and data (* means that data is transmitted on the over-the-air interface).....	54
Figure 4-45: C9 - Messages sequence chart. ....	54
Figure 4-46: C9 - Time diagram.....	55
Figure 4-47: Position estimation RMSE of proposed approach of C9 (ANM) over transmit power $P$ , compared to the theoretical CRLB. $T$ means the number of pilot packets required. ....	56
Figure 4-48: The effect of the number of BS antennas $N$ and that of RISs $M$ on the performance of the proposed 3D localisation system (ANM) and the theoretical CRLB over transmit power $P$ . ....	56
Figure 4-49: C10 - Physical deployment vs. architecture requirements of [VRK+22], in terms of control signalling and data (* means that data is transmitted on the over-the-air interface). ....	57
Figure 4-50: C10 - Messages sequence chart. ....	58
Figure 4-51: C10 - Time diagram.....	58
Figure 4-52: Exemplary human detection with fixed RIS aperture of $M = 259 \times 259$ , in a $\gamma = 0$ dB condition, with $S = 100$ averaging strategy, $U_a = 20$ active users and $U_p = 10$ passive users in the scenario. ....	59
Figure 4-53: Average human detection percentage (%) and positioning errors (cm) with fixed RIS aperture of $M = 259 \times 259$ , in a $\gamma = 0$ dB condition, with $S = 100$ averaging strategy and $U_p = 10$ passive users in the scenario for different numbers of active devices $U_a$ . ....	59
Figure 5-1: Simplified block diagram of the RIS-enabled mmWave VNA-based channel sounder, with 1-bit R-RIS phase control, used for offline validations of RIS-enabled single-BS localisation feasibility. ....	61
Figure 5-2: Layout and deployment information of the reference indoor environment considered for the mmWave channel measurement campaign and the related RIS-aided positioning experiments, incl. 1 BS location, 2 R-RIS locations (R-RIS 1 and 2) and 5 UE locations (UE1 to UE5). ....	62
Figure 5-3: Analog and digital components of the FMCW radar at the UE.....	64
Figure 5-4: Demonstration of the testbed and components for the FMCW radar-RIS pair. ....	64
Figure 5-5: Principle of the online field trial for single-BS RIS-aided single-BS localisation within commercial network (the so-called “trial” locations correspond to the tested candidate UE locations). ....	67
Figure 6-1: Physical architecture requirements in terms of control signalling for all the proposed localisation and sensing schemes. ....	68



Document:	H2020-ICT-52/RISE-6G/D5.3		
Date:	30/06/2023	Security:	Public
Status:		Version:	1.0

## List of Tables

Table 4-1: Overview of the architecture proposals for localisation and sensing (columns with the same colour rely on a similar physical deployment, while stars * in the “Architecture” rows denote the physical entities to be located).....	26
Table 5-1: Main characteristics of the R-RIS used for demonstrating RIS-enabled single-BS localisation. ....	61
Table 5-2: Tested positioning scenarios (DP: Direct path, RP: RISx-reflected path on R-RISx); Expected RIS benefits: * vs. conventional single-BS positioning using also RSS measurements, ** vs. conventional single-BS positioning with similar MPCs estimation capabilities but relying on DP only, *** vs. conventional single-BS positioning with similar MPCs capabilities, but relying on DP only or with no extra SLAM capabilities.....	63
Table 6-1: Considered proposals related to RIS control for localisation and sensing.....	68



---

Document:	H2020-ICT-52/RISE-6G/D5.3		
Date:	30/06/2023	Security:	Public
Status:		Version:	1.0

---

## List of Acronyms

3GPP	3rd Generation Partnership Project
5G-NR	5 <sup>th</sup> Generation - New Radio
5G-PPP	5G infrastructure Public-Private Partnership
ACK	Acknowledgement
ADC	Analog to Digital Converter
AMF	Access and Mobility management Function
ANM	Atomic Norm Minimisation
AoA	Angle of Arrival
AoD	Angle of Departure
AP	Access Point
BS	Base Station
CDF	Cumulative Density Function
CR(L)B	Cramér-Rao (Lower) Bound
CSI	Channel state information
CU	Centralised Unit
DB	Database
DL	Downlink
DoA	Direction of Arrival
DoD	Direction of Departure
DP	Direct Path
DU	Distributed Unit
EMF	Electromagnetic Field
eNb	evolved Node b
ETSI	European Telecommunications Standards Institute
FF	Far-field
FFT	Fast Fourier Transform
FMCW	Frequency Modulated Continuous Wave
gNb	Next generation Node b
KPI	Key Performance Indicator
LMF	Location Management Function
LoS	Line-of-Sight
MAE	Mean Absolute Error
MC	Multicarrier
MCU	Microcontroller Unit



---

Document:	H2020-ICT-52/RISE-6G/D5.3		
Date:	30/06/2023	Security:	Public
Status:		Version:	1.0

---

MEC	Multi-Access Edge Computing
MIMO	Multiple Inputs Multiple Outputs
MPC	multipath components
MUSIC	MUltiple SIgnal Classification
near-RT RIC	near Real-Time RAN Intelligent Controller
NF	Near-field
NFV	Network Function Virtualisation
NLoS	Non-line-of-sight
NSA	Non-Standalone
NUE	Non-intended user
NR	New Radio
ODU	Outdoor Unit
OEB	Orientation error bound
OFDM	Orthogonal Frequency Division Multiplexing
OMP	Orthogonal Matching Pursuit
O-RAN	Open - RAN
PCB	Printed Circuit Board
PEB	Position error bound
RAN	Radio Access Network
RF	Radio Frequency
R-RIS	Reflective RIS
RT-RIS	Reflective-Transmissive RIS
RIS	Reconfigurable Intelligent Surface
RISA	RIS actuator
RISC	RIS controller
RISO	RIS orchestrator
RMSE	Root Mean Square Error
RP	Reflected Path
RSRP	Reference Signal Received Power
RSS(I)	Received Signal Strength (Indicator)
R-RIS	Reflective RIS
RTT	Round Trip Time
Rx	Receiver
SAGE	Space-Alternating Generalized Expectation-maximization
SINR	Signal-to-interference and noise ratio



---

Document:	H2020-ICT-52/RISE-6G/D5.3		
Date:	30/06/2023	Security:	Public
Status:		Version:	1.0

---

SISO	Single Input Single Output
SLAM	Simultaneous Localisation and Mapping
SNR	Signal-to-noise ratio
TDofA	Time Difference of Arrival
TEMS	Test Mobile System
ToA	Time of Arrival
T-RIS	Transmissive RIS
Tx	Transmitter
UE	User equipment
UL	Uplink
UL-DoA	Uplink Direction of Arrival
UL-TDoA	Uplink Time Difference of Arrival
VNA	Vector Network Analyser
WP	Work package



Document:	H2020-ICT-52/RISE-6G/D5.3		
Date:	30/06/2023	Security:	Public
Status:		Version:	1.0

## 1 Introduction

The RISE-6G project is one of the Fifth-Generation infrastructure Public-Private Partnership (5G-PPP) projects under the European Commission’s Horizon 2020 framework. The focus of the project is to design, prototype, and trial radical technological advances based on reconfigurable intelligent surfaces (RISs) to forge a new generation of dynamically programmable wireless propagation environments. RISs are expected to both enable and boost connectivity, localisation, and sensing performance, as well as to timely adapt to dynamic requirements on electromagnetic field emissions, energy efficiency, and secrecy.

Within RISE-6G, work package 5 (WP5) considers exploiting the RIS technology for improved localisation, sensing and mapping performances more specifically. To this end, the expected contribution of WP5 is two-fold: (i) determining suitable RIS-augmented network deployments and RIS control mechanisms optimising localisation-oriented key performance indicators (KPIs); (ii) developing and evaluating the necessary detection and estimation algorithms that enable RIS-based localisation and sensing. It concerns not only the localisation of connected user devices, but also that of passive objects (incl. non-connected users), and beyond, the construction of dynamic physical and/or radio maps of the environment.

### 1.1 Deliverable objectives

As an update of D5.1 [RIS5.1-22], this new D5.3 document, which is entitled “Control for RIS-based localisation, mapping and sensing (Final Specifications)”, summarizes the final results issued in the context of the first task of WP5. More particularly, it reports a variety of physical architectures and RIS control strategies (typically, at beam or unit cell levels), which also come along with supporting data flows and signalling schemes. The latter can differ from those needed to support communication. Among all these proposals, the choice of a particular setting depends on the application scenario (e.g., localisation of a connected user equipment, a mobile RIS, a passive obstacle, etc.), as well as on operating constraints (e.g., number of active base stations, visibility conditions, proximity to the RIS, synchronisation, etc.). From that perspective, D5.3 is deliberately intended to cover a large span of concrete cases and solutions, where RISs are expected to be beneficial to localisation and sensing.

Leveraging the RISE-6G architecture vision and terminology initially introduced in D2.5 [RIS2.5-22], a discussion is also herein carried out on how location-oriented application requirements (e.g., latency, refreshment rate, accuracy...) impact both the partitioning and the execution of the new logical functions involved in the RIS-augmented network architecture. Together with other parallel deliverables D4.3 and D6.3, this D5.3 will thus serve as input material towards the final definition of a unified RISE-6G architecture in WP2 by the end of the project. In particular, it will contribute to specify the common logical blocks, as well as their interfaces.

Last but not least, another objective of this D5.3 is to identify among all these proposed WP5 solutions a few representative deployment scenarios and RIS control candidates for possible experimental validations under real hardware constraints in the frame of WP7 (i.e., through in-laboratory demonstrations or field trials).

### 1.2 Deliverable structure

The rest of the document is structured as follows. Section 2 reviews the basics of localisation and sensing, comparing conventional and RIS-aided approaches. This section also recalls the main performance metrics and indicators in use in other sections, along with a few elements regarding the performance evaluation methodology. Section 3 motivates the need for dedicated architectures, control mechanisms, as well as protocols, while emphasising their main challenges in light of RIS-aided localisation and sensing applications. Then Section 4 details ten original proposals, including both deployment and control aspects. More precisely, for each solution, the corresponding deployment scenario and its physical architecture requirements, the signalling scheme, and the data flow (by means of indicative message sequence charts and time diagrams) have been described. Section 5 draws the list of the physical architectures and control



Document:	H2020-ICT-52/RISE-6G/D5.3		
Date:	30/06/2023	Security:	Public
Status:		Version:	1.0

approaches selected for experimental validation in WP7. Finally, Section 6 concludes the deliverable and provides some recommendations regarding the final RISE-6G architecture.

### 1.3 Disclaimer on RISE-6G architecture definition with respect to project timeline.

RISE-6G project builds a new architecture for RIS-enabled networks with the following stepped approach:

- Step 1: during the first half of the project, WP4/5/6 have reported intermediary requirements in terms of architecture and control signalling to support their innovations, in D4.1 [RIS4.1-22] / D5.1 [RIS5.1-22] / D6.1 [RIS6.1-22], respectively.
- Step 2: all the aforementioned requirements have been used to derive an intermediary RISE network architecture in D2.5 [RIS2.5-22].
- Step 3: During the second half of the project, D4.1 [RIS4.1-22] / D5.1 [RIS5.1-22] / D6.1 [RIS6.1-22] are updated to D4.3, D5.3 and D6.3) to report the final requirements in terms of architecture and control signalling, taking into account latest and additional innovations.
- Step 4: at M30 of the project, almost all HW RIS prototypes of the project are made available to the consortium. The project lists the different practical ways to control a RIS. The project lists the different practical ways to split the control of the RIS in a functional and physical architecture.
- Step 5: D2.6 provides the final RISE network architecture, taking into account:
  - o requirements on architecture and control signalling to support innovations from WP4/5/6, from step 3;
  - o the analysis of practical splits based on existing RIS prototypes, from step 4;

As a consequence, the concepts linked to the split of control in the functional and/or physical architecture, such as RIS actuator (RISA), RIS controller (RISC) and/or RIS Orchestrator (RISO), will reach their final definitions only in step 5.

Before that step is taken, the definitions of these concepts are local to each deliverable preceding D2.6, and may vary between deliverables preceding D2.6.

## 2 Localisation and sensing basics

As in the previous deliverables, [RIS5.1-22, RIS5.2-22], a brief overview of the principles of radio localisation and sensing, with an emphasis on cellular approaches is now provided. Then the general use of RISs in the context of localisation and sensing will be detailed, followed by a discussion on the corresponding need for architectures and control methods.

### 2.1 Foundations of localisation

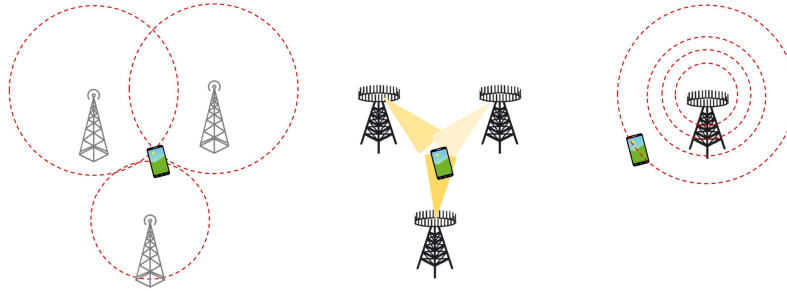
Radio localisation (synonym: positioning) is the process of determining the location of a connected device (a user equipment (UE)), based on uplink (UL) or downlink (DL) measurements with respect to several base stations (BSs) [PRL+18]. The measurements can take on the following forms:

1. *Time measurements*: The most common types of measurements are derived from the time-of-arrival (ToA) in UL or DL. When at least 4 such measurements are available from 4 synchronized BSs with known location, the UE 3D location and clock bias can be determined. When the BSs are not synchronized, the round-trip-time (RTT) with respect to each individual BS should be computed, which can be directly transformed into a distance. When RTT measurement with respect to 3 BSs are present, the 3D UE location can be computed. This is shown in Figure 2-1 (left).
2. *Angle measurements*: Another common type of measurement is DL angle-of-departure (AoD) or UL angle-of-arrival (AoA), which requires a multi-antenna BS. When each BS is equipped



with a planar array, a UE can determine its 3D location from angle measurements (in azimuth and elevation) with respect to 2 BSs, provided their locations and orientations are known. This is shown in Figure 2-1 (middle). Note that angle measurements at the UE side are also possible but are harder to utilize for localisation as the UE orientation is generally unknown.

3. *Position measurements*: A less common measurement, but important in the context of this work, is a direct position measurement. Such measurements are possible when the observed DL or UL signal cannot be expressed only in function of angles and delays, for example in near-field (NF) scenarios. NF measurements require extremely large arrays, but allow 3D localisation with a single BS. This is shown in Figure 2-1 (right)
4. *Other types of measurements*: Other types of measurement such as Doppler measurements, or the extraction features as input to machine learning methods are also possible. Doppler measurements by themselves are insufficient for positioning. On the other hand, in rich scattering environments, waveform features from a single BS are sufficient to determine the UE 3D location.



**Figure 2-1: Example of RTT-based localisation (left), constraining the UE on the intersection of circles (2D) or spheres (3D); localisation based on DL-AoD measurements (middle), constraining the user within a sector of each BS; localisation based on near-field measurements exploiting the wavefront curvature (right).**

Localisation quality depends inherently on the quality of the underlying measurements. The quality of these measurements depends on [WLW+18]: the available resolution (i.e., the ability to separate multipath in either delay or angle), the signal-to-noise-ratio (SNR), the propagation channel (which in turn depends on the operating frequency), and the models of the end-to-end channel, including the propagation channel and the hardware of the transmitter and receiver. Accurate localisation requires high resolution, sufficient integrated SNR, as well as a benign channel (a sparse channel for model-based signal processing and a rich channel for machine learning positioning), and good knowledge of the end-to-end channel. If any of these factors is missing, localisation accuracy will suffer.

Even with good quality measurements, localisation quality is also a function of the deployment, which refers to the geometric placement of the BSs. A good deployment allows a UE in the coverage zone to have a line-of-sight (LoS) link to at least 4 well-separated BSs, when ToA measurements are utilised.

## 2.2 From localisation to sensing

Sensing in general involves the detection and estimation of changes or events in the environment from observed radio signals. Sensing is often limited to radar-like sensing, i.e., detection and tracking of passive objects. In contrast to localisation, 3GPP has until now not offered any support for radar-like sensing. Nevertheless, localisation and sensing are closely linked, as localisation is a special case of bistatic or multi-static sensing, in which the non-line-of-sight (NLoS) paths are ignored. In general sensing harnesses all resolvable paths to map passive objects or track passive targets. A visual representation of different forms of radar-like sensing is provided in Figure 2-2. For a more detailed description, the reader is referred to [RIS5.2-22].

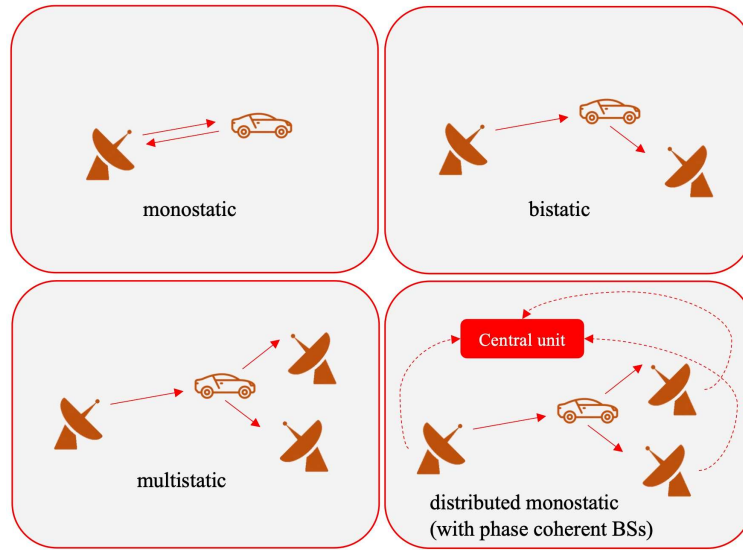


Figure 2-2: Different form of sensing.

### 2.3 RIS-aided localisation and sensing

RISs have the potential to improve localisation and sensing performance, when added to conventional deployments [WHD+20]. This is referred to as ‘boosting’. In addition, RIS also have the potential to provide location estimates to UEs when conventional deployments fail. This is referred to as ‘enabling’. The discussion in this section is mainly limited to passive or reflective RISs, as they have the most limited capabilities. Other forms of RIS, such as active RIS (which can amplify the reflected signal), hybrid RIS (which can locally process the impinging signal), or simultaneously transmitting and reflecting RIS (STAR RIS) have more extensive capabilities and will thus naturally lead to better localisation and sensing performance.

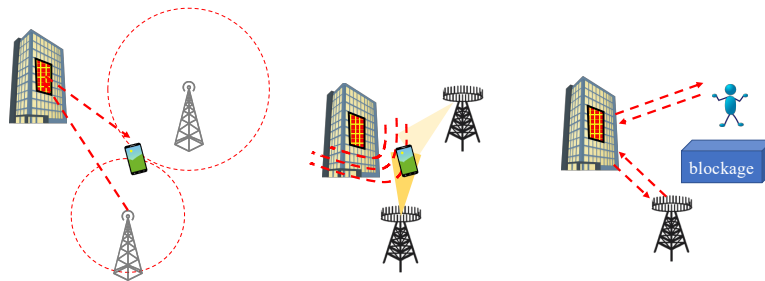


Figure 2-3: Examples of use of RIS in localisation: a new signal path via a RIS and a new reference by the RIS (left); large RIS provides wavefront curvature for localisation measurements (middle); a RIS provides a signal path to avoid signal blockage in monostatic sensing [RIS5.2-22].

In wireless systems, RISs can boost or enable user localisation by providing the following (see Figure 2-3). First, each RIS provides *new location-dependent measurements* from which angles and delays or (in the case of near-field) locations can be computed. Since the RIS paths can be controlled, they can be optimised to maximise the accuracy of these measurements. Secondly, each RIS can *act as a location reference*, provided its location and orientation are known. Hence, the measurement can be directly used in a similar way as measurements from a BS.



Document:	H2020-ICT-52/RISE-6G/D5.3		
Date:	30/06/2023	Security:	Public
Status:		Version:	1.0

## 2.4 Key performance indicators and their evaluation

### 2.4.1 Localisation and sensing performance metrics

An exhaustive overview of all relevant localisation and sensing metrics is beyond the scope of this document. For this purpose, the reader is referred to e.g., [ZGL19]. The most important metrics for this document, as already reported in D2.4 [RIS2.4-22], are:

- *Accuracy*: this metric typically refers to the norm of the location error that can be achieved a certain fraction (e.g., 90% or 99%) of space and/or time. Evaluating the localisation accuracy thus requires collecting error statistics in the deployment region over time.
- *Coverage*: The region of space for which the localisation / sensing error is below a certain threshold value.
- *Availability*: The fraction of time for which the localisation / sensing is available (providing a certain quality of service).
- *Latency*: The latency refers to the time between the request of location update and receiving the update, in which case it comprises control signalling, computation, and transmission and reception of the radio signals.

### 2.4.2 Methods and evaluation

To evaluate the localisation / sensing metrics above, several approaches are considered by RISE-6G, ranging from theoretical bounds, simulations with different levels of accuracy, up to system experiments.

- *Theoretical performance bounds*: the position error bound (PEB) is a theoretical tool that can predict the best localisation accuracy, provided some technical conditions hold. The PEB is thus also a way to compare different deployments without the need to develop working algorithms. The theoretical performance bounds require accurate models of the propagation channel and hardware for the performance predictions to be accurate.
- *Simulations*: Once practical algorithms have been developed, they can be tested on synthetic data generated with the help of the accurate channel and hardware models. The evaluation of accuracy levels practically relies on the empirical localisation estimation error, which is obtained over multiple simulation trials while introducing randomness between these successive trials (e.g., in terms of noise realisations and/or tested positions, etc.), depending on the considered scenario. Simulation studies can provide a more refined picture of the accuracy, coverage, and availability, but usually, they cannot accurately capture latency.
- *Experiments*: The final step taken in RISE-6G is the practical demonstration of localisation / sensing with RIS at different frequency bands. An important difference with simulations is that experiments need a ground-truth system in order to compute the localisation errors.

This D5.3 deliverable focuses mainly in theoretical performance bounds and simulations in Section 4, while aspects related to experiments, which are just briefly alluded in Section 5, will be much more detailed in next WP7 deliverables.

## 3 Motivations for new architectures and control schemes in RIS-aided localisation and sensing

### 3.1 Architectures for RIS-aided localisation and sensing

The envisioned RISE-6G architecture includes three main logical components that are involved in configuring and using the RIS as a system component, namely a RIS orchestrator, a RIS controller and a RIS actuator. In the architecture-related considerations that follow, the main emphasis is on the possible mapping between physical entities and these logical functions, as well as on information flow, and signalling



Document:	H2020-ICT-52/RISE-6G/D5.3		
Date:	30/06/2023	Security:	Public
Status:		Version:	1.0

needs. The outlined architectures are expected to be directly applicable in a single operator case but needing further evaluation in a multi-operator case. Eventually, the envisioned architectures also need to be evaluated for compatibility within the 3GPP framework.

### 3.1.1 General RISE-6G architecture proposal

RIS is a new network element and its integration into the network infrastructure requires a structured approach that defines both the roles of the RIS as well as the protocols between the RIS and the rest of the system [DZD+20]. The RIS phase configuration controls the physical observation that positioning is based on, and thereby any positioning strategy either requires the explicit control of the RIS configuration or must operate with the knowledge of the RIS configuration in use. However, the architecture must also consider that the RIS is envisioned as a multi-purpose element, used for communication, sensing, and positioning.

As a starting point, the global RISE-6G architecture initially envisaged in [RIS2.5-22] includes the following logical components:

- **RIS**: it is the device based on reflect-array or meta-material technology that is directly controlled by an associated RIS actuator. In some scenarios, the RIS actuator may be embedded into the RIS device. In such a case, we envision a resulting new RIS device directly controlled by the RIS controller (RISC) function.
- **RIS actuator (RISA)**: it is the element in charge of actuating the logical commands received by the RISC, i.e., of translating them into physical configurations to be applied to the RIS device. In particular, such configurations might be envisioned as phase shifts or ad-hoc meta-material state changes. In addition, the RIS actuator can provide feedback or limited sensing input when considering different RIS devices. The RISA is controlled by the RISC.
- **RIS controller (RISC)**: the controller associated to an RIS actuator or an RIS function. It is responsible for generating the logical commands associated to the switching operations between the configurations/states of the RIS elements (e.g., predefined phase shifts); RISCs may have different levels of complexity and capabilities and can embed third-party apps to implement smart algorithms. An RISC may either be controlled by other elements in the network, in which case it simply acts as an interface that configures the RIS elements based on external explicit instructions (Controlled RIS), or it may operate on its own (Autonomous RIS).
- **RIS orchestrator (RISO)**: the orchestrator is placed on a higher (hierarchical) layer and it coordinates multiple RISCs.

The previous taxonomy is ordered according to increasing complexity and computational capabilities (but also, time granularity). Unless otherwise stated, we refer to RIS as the overall device, thus implying that optimization and control functions are carried out at the RISC and RISA depending on the required time granularity and computational complexity. As already mentioned above, the definitive definitions and interfaces of RISA/RISC/RISO blocks are left to the final deliverable D2.6.

### 3.1.2 Specific requirements and challenges in RIS-aided localisation and sensing

A RIS-aided localisation architecture should support the collection of measurements at the BS and/or UE, the application of adequate RIS configurations during measurements collection, as well as synchronisation of these with the transmission of pilots by the BS or UE. Localisation algorithms will typically require knowledge of (or also control over) the RIS configurations utilised during the measurements collection, as well as the measurements themselves. Therefore, the localisation algorithms can be envisioned performed in either the RIS controller or the measurement point, whereas other choices for computation execution require both the RIS configuration and measurements as inputs.

In comparison with localisation embodiments, a sensing architecture has one more requirement: it must indeed support the collection of measurements in a RIS-centric system. This may be done, as in most of



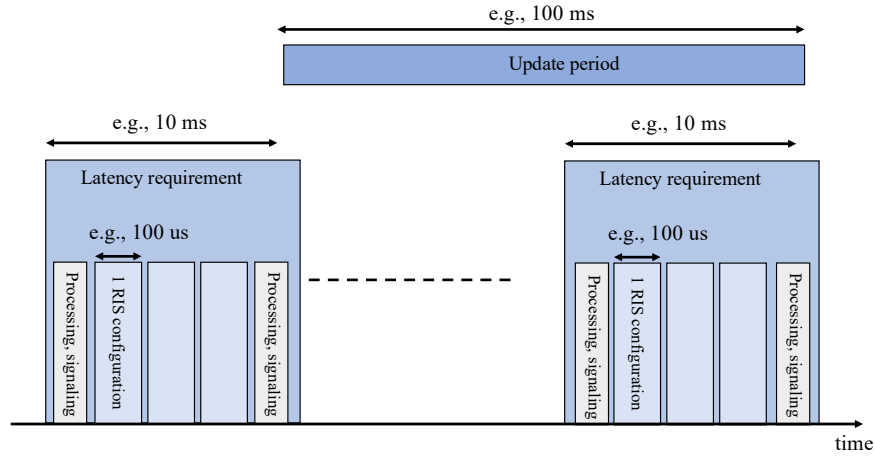
Document:	H2020-ICT-52/RISE-6G/D5.3		
Date:	30/06/2023	Security:	Public
Status:		Version:	1.0

the envisioned contributions, directly by the RIS, either in sampled or sampled and pre-processed base-band format. If observations at the BS will be relevant for sensing, they should be supported by the architecture. In sensing approaches, the data flow is usually one way, from UE to the network side (typically leveraging UL signals). The network side then collects the information with the endpoint being at the physical RIS. The necessary signalling includes only the RIS configuration and related timing control.

From a localisation and sensing standpoint, the relationship between the deployed physical entities and the logical components/functions of the architecture is strongly impacted by a priori application requirements, as well as by the computational complexity affordable at each of these physical entities (typically at the RIS device).

The different components of the RISE-6G architecture indeed operate at different time scales, so that they have a close relation to the localisation / sensing *latency*. The latency itself is upper bounded due to the mobility and the accuracy requirement. Roughly speaking, an accuracy requirement of  $E$  meters and a mobility of  $V$  meter/second has a tolerable latency of around  $0.1E/V$ . The latency is distinct from the refresh period, which may be on the order of tens of ms to several seconds, depending on the available external sensors and fusion mechanisms. With these considerations in mind, the following applies (see also Figure 3-1):

- A localization refresh period on the order of 100 ms is usually suitable to most mobility regimes (typically, like GPS readings every 100 ms).
- Once requested, the overall localisation process should be sufficiently timely to avoid that the UE has travelled a too large distance during acquisition. In practice, localization shall hence be completed within 10 ms typically, which supports cm-level accuracy at low velocities ( $< 1$  m/s, e.g., indoors) and m-level accuracies at high mobility (around 10 m/s, e.g., outdoors).
- In scenarios requiring more than one RIS, the RISO serves (more or less) as a scheduler, which oversees orchestrating all the beam operations at the different RISs involved in localisation and sensing. Typically, every 100ms, RISO then selects and triggers clusters of RISs that must perform their tasks within 10 ms (e.g., beam scanning).
- In terms of logical RIS control, these high-level tasks may be split into more elementary tasks (e.g., beam selection in a pre-defined localisation-optimal sequence), which are performed by the RIS controller that is either co-located with the BS (on the network side), or hosted at the physical RIS itself, depending on the computational capabilities of the latter. Finally, the most elementary operations (i.e., that with finest time granularity) are carried out at the RIS itself through its RIS actuator (e.g., loading of the requested RIS configuration).
- To produce one single location estimate, the RIS configuration needs to be changed depending on the kind of processing:
  - ***In non-coherent processing***, the RISs generate directional beams, which in turn are used to derive AoA or AoD (e.g., based on signal strength) and ToA (based on the strongest beam). The plurality of RIS beams should be generated within the latency budget. For instance, if 2 RISs cooperate to localise a user, and each RIS uses 20 beams, then the beams should be changed every 250  $\mu$ s, given a latency budget of 10 ms.
  - ***In coherent processing***, the RIS update period depends mostly on the channel coherence time, and hence, on operating frequency, since phase-coherent integration and processing is performed. At a carrier frequency of 3 GHz and a velocity of 1 m/s, the coherence time is approximately 100 ms, while at 30 GHz, the coherence time drops to 10 ms. All RIS configurations must hence have been executed within this coherence time.



**Figure 3-1: Localisation and sensing time scales.**

Note that the interfaces between different logical architecture components involved in the main localisation-oriented RIS control proposals detailed hereafter in Section 4 will be fully specified in upcoming D2.6 deliverable.

### 3.2 Control schemes for RIS-aided localisation and sensing

To devise control schemes aimed for localisation and sensing, the following aspects need to be considered: the sensing and computational entities of the environment, the types of measurements and their acquisition process, the configuration of the RIS, and the collection point of the localisation or sensing information, while accounting for hardware capabilities and potential limitations of the available hardware, and in particular the hardware of the RIS. It is important to highlight that the challenges of determining effective control schemes are made specific by the inclusion of the reconfigurable surfaces and require a careful reinvestigation of existing schemes. The contributions presented in this D5.3 (see Table 4-1) are detailed in a way that addresses these considerations. In the following, the specific components of the control schemes are discussed:

- **Computational and sensing entities:** Traditionally, the entities that are capable of sensing the RF signals and perform the computation are the BS(s) or the UE(s). With the inclusion of a RIS, more intricate schemes can be devised. When passive, purely reflecting, surfaces are deployed, the sensing entities remain the same. However, when RISs are endowed with additional sensing or transmissive capabilities, multiple network components can play the role of sensors, resulting to more elaborate strategies. When the metasurface is also capable of standalone computation, i.e., when the RISC or RISO entities are physically located onto the RIS, the surface may also perform part or the complete computational procedures needed under the localisation scheme, which has the potential to greatly simplify the architectural, computational, and signalling requirements of the network. Under this deliverable, proposals C3, C4, C7, C8, and C10 explore the concepts of sensing- and computationally-empowered RISs.
- **Measurement acquisition:** As a prerequisite, the type and acquisition process of measurements is inherently linked to the implementation of any control scheme. Different strategies may be based on various kinds of sensed RF signals from the environment to the extent that such considerations play an important role on the nature of the control, while simultaneously affecting the architectural, algorithmic, and computational requirements. Concretely, the contributions of Sec-





---

Document:	H2020-ICT-52/RISE-6G/D5.3		
Date:	30/06/2023	Security:	Public
Status:		Version:	1.0

---

tion 4 involve measurement types which include RTTs, CSI, DoAs or Radio Maps. The estimation of such informative indicators is not always a trivial task, and therefore, it is part of the complete specification of each of the control schemes.

- **Example:** the collection of Channel State Information (CSI) matrices is not trivial under localization and sensing. For data communication purposes, this problem can be solved through the estimation of cascaded channel responses by using successive pilots and varying the RIS configurations over pilot transmissions. Then the cascaded channel can be recovered, for instance by least-squares estimation [SZL+21]. However, in case of RIS-based localisation, this approach might be suboptimal depending on the specific localisation scenario (e.g., DL/UL transmissions, 2D/3D, estimated radio metrics available as observations, near-field/far-field regime, targeted state variables). For instance, simpler random RIS phase profiles could enable asynchronous positioning in downlink single-input-single-output (SISO) multi-carrier (MC) transmission contexts, while many successive transmissions are needed. This scheme does not require any prior information (neither about the channel, nor about the UE location), but it is not optimal under a priori UE location information.
- **RIS configuration methodologies:** For data communication, concentrating power towards the user to be served and accordingly, concentrating signal-to-interference-and-noise-ratio (SINR), is a meaningful approach to optimise communication rate. For localisation and sensing, RIS profiles (typically, phase profiles) can be configured to optimise the static PEB (and/or the orientation error bound (OEB)), even in more generic multiple inputs multiple outputs (MIMO) MC contexts, based on the prior UE location. In this case however, the actual uncertainty regarding this prior knowledge in a real system (typically, while using the latest known location estimate instead of the perfect knowledge, along with its covariance) can be incorporated by design in the optimisation problem.

While a number of control techniques for RIS-aided localization and sensing do involve solving optimisation problems, other control schemes rely on different kinds of techniques for RIS configuration, such as selection of beams from codebooks (that are either designed specifically for localisation or are more general-purpose), selecting arbitrary, or even random configurations, to the purpose of alleviating the demanding computational procedures associated with RIS-optimisation.

- **Hardware impairments:** Real RIS hardware limitations shall be considered in the control design too. In general, there exist several theoretical models for phase control, quantised phase control, amplitude-dependent phase control, and joint amplitude and phase control, which all require tailored optimisation. Another unified way of treating these models consists in relying on lookup tables instead, which list all realisable amplitudes and phases in practice at each element with a given RIS hardware. Such tables can also account for coupling effects, which are challenging to treat analytically. All in all, the optimisation of RIS configuration (based on real lookup tables or more conventional model-based descriptions) could hence be performed prior to or after constraining the problem by real hardware capabilities, potentially with a strong impact onto performance (e.g., in terms of beam peak power, achievable beam shape, secondary lobes). Under this deliverable, contributions C5 and C6 are designed to specifically address the problems of hardware impairments and limitations.
- **Localisation-information collection points:** As a final consideration of control schemes, the collection point of the end-result needs to be considered. Again, in traditional UL/DL communications the information resulting from the computational entities typically resides on the nodes receiving the signals. As mentioned above, when receiving and computationally able RISs are envisioned, the information may be generated within the surface, therefore requiring a dedicated



Document:	H2020-ICT-52/RISE-6G/D5.3		
Date:	30/06/2023	Security:	Public
Status:		Version:	1.0

(though low throughput) control/feedback channel for that information to be transmitted to the interested entity.

From the above discussion, an effective control scheme needs careful consideration. Indeed, it is one of the fundamental pillars for successful RIS-aided localisation and sensing, alongside the architectural aspects (Section 3.1), the signalling structure (Section 3.3) and algorithmic techniques (which is the primary focus of upcoming D5.4). For clarity, the above control considerations are explicitly detailed for each of the technical proposals of the current deliverable presented in Table 4-1.

### 3.3 Signalling and protocols for RIS-aided localisation and sensing

Due to the unprecedented control over wireless propagation they offer, RIS can be employed to enhance (or enable) localisation and sensing capabilities in wireless systems. However, to fully exploit the potential of RIS, it is important to consider signalling procedures and protocols which are essential to its operation. In particular, the introduction of the RIS (being a new network element) and the novel algorithms associated with it need to be analysed from the point of view of the existing infrastructure, to identify potential challenges in terms of future implementation and integration.

#### 3.3.1 RIS signalling

The incorporation of RIS in wireless systems introduces additional signalling overhead. Most notably, signalling is necessary to convey the control information to the RIS, allowing it to adjust the reflection coefficients of its elements at specified times. Furthermore, additional synchronization signals and procedures to facilitate the exchange of localization/sensing data might be required. Last but not least, certain localization and sensing algorithms might call for specific signals to initiate, terminate or acknowledge the exchange between BS, RIS and UE.

#### 3.3.2 RIS protocols

In recent research and state-of-the-art literature, the focus is usually on the newly developed methods themselves, which are supposed to enable novel RIS-aided tasks or functionalities. Depending whether it is about localization, sensing or communication, the attention has thus been paid mostly to the algorithms these new tasks are based on, as well as to their performance. While this is no doubt crucial, it is also important to consider the protocol side of any proposed algorithm and how it fits into the existing systems - its impact on other processes (e.g. data exchange, CSI acquisition) in terms of resource allocation, whether it requires introducing new signals or can reuse existing ones. The latter is particularly important in the context of control signalling mentioned earlier. Lastly, since the localization information can be used in other procedures such as channel estimation and beam management, it is desirable to consider comprehensive protocols to assess their latency requirements and feasibility.

In this D5.3 deliverable, we delve into those, often overlooked, issues by explicitly considering the minimum signalling requirements, necessary logical connections between entities, and time diagrams for each localization/sensing method proposed. Ultimately, the development of standardized signalling procedures and protocols will foster the widespread adoption of RIS in wireless systems, paving the way for enhanced localisation and sensing capabilities in future wireless communication networks.

## 4 RISE-6G architecture and control proposals for RIS-aided localisation and sensing

All the proposals below feature RISs as connected devices. This does not mean that the RIS itself is necessarily endowed with full-extent communication capabilities, but only that it is equipped with suitable hardware and interfaces to receive and send only the required (control) messages.





#### 4.1 Summary of RISE-6G proposals

The table below summarizes the main proposals from RISE-6G WP5 for localisation and sensing, focusing on physical architecture and deployment, control (at beam or unit cell levels) and signalling aspects. In the following subsections, we detail further each of these proposals.

RISE-6G Contributions	C1	C2	C3	C4	C5	C6	C7	C8	C9	C10
<b>Architecture</b>										
Nr BS	1	$\geq 2$ (2D) $\geq 3$ (3D)	0	0	1	1	0	0	1	1
Nr RIS	1 (LOS), $\geq 2$ (NLOS)	1*	1 (RTT and AOD) 3-4 (RTT only)	1	1	1	$\geq 3$	1	$\geq 2$ (NLOS)	1
Nr UEs	1*	0	1*	$\geq 2$ *	1*	1*	1*	1*	1*	$\geq 1$ *
UE Mobility	Static	Mobile	Static	Static	Static	Static	Static	Static	Static	Static
RIS Type	Reflect. (Passive)	Reflect. (Passive)	Reflect. (Passive)	Reflect. (Passive)	Reflect. (Passive)	Reflect. (Passive)	Receiv. (Hybrid)	Receiv. (Hybrid)	Reflect. (Passive)	Receiv.
Nr non-connected targets	0	0	0 for localisation, $\geq 1$ * for mapping	0	0	0	0	0	0	$\geq 1$ *
Localization functionality placement	At UE (or BS)	At BS	At UE	At UE	At UE (or BS)	At UE (or BS)	At RISC	At RISC	At BS (also RISC)	At RISC
<b>Setup</b>										
Indoor/outdoor	Indoor (short range)	Outdoor (multi-BS)	Indoor or outdoor	Indoor or outdoor (e.g., V2V)	Indoor (short range)	Indoor (short range)	Indoor	Indoor	Indoor or outdoor	Indoor or outdoor
2D/3D	3D	2D/3D	3D	3D	3D	3D	3D	3D	3D	2D
Frequency Band	Preferably mmWave	Any	Preferably mmWave or even sub-THz	mmWave	Preferably mmWave	Preferably mmWave	Any	Any	Any	Any
Near field/far field	FF	NF/FF	FF	FF	NF/FF	NF/FF	FF	FF	FF	NF/FF
LOS/NLOS/Both	LOS	BS-BS LOS (+RIS-reflected paths)	LOS (+ NLOS for mapping)	UE-UE LOS (+RIS-reflected paths)	LOS/ NLOS	NLOS	LOS/ NLOS	LOS	NLOS	LOS
Hardware considerations	None	None	Full-Duplex UE needed	None	Large surface	Large surface + Lookup tables of element-wise reflection coefficient needed	None	Partially connected RIS (with several RF chains)	None	Large surface
<b>Data flow &amp; Signalling</b>										
Uplink/Downlink	UL or DL	DL and UL	UL	UL	DL	DL	UL	UL	UL	UL
Measurement type	AOD and Delay in LOS WB (or several AODs in NB and/or in NLOS)	Delays (+ optional AOA/AODs if TxBSs and RXBSs have multiple antennas)	RTT and RIS AOD	Delays (+ optional AOA/AODs)	Position directly from IQ samples	Position directly from IQ samples	AOD at each RIS	Several AODs at the RIS	AOAs from RIS-reflected paths	Radio map (Matched filter output)
RIS configuration strategy	Arbitrary or location-based / Several	Random / Several profiles needed	Arbitrary or location-based / Several profiles needed	Arbitrary or location-based / Several profiles needed	Location-based / Several profiles needed	Location-based / Several profiles needed	Arbitrary / Several profiles needed	Arbitrary / Several profiles needed	Random / Several profiles needed	Arbitrary



Document: H2020-ICT-52/RISE-6G/D5.3  
Date: 30/06/2023 Security: Public  
Status: Version: 1.0

	profiles needed									
Who collects measure- ments	UE (DL) or BS (UL)	BS	UE	UE	UE	UE	RIS	RIS	BS	RIS
Narrow- band/wide- band	WB or NB	WB	WB	WB	WB or NB	WB or NB	NB	NB	NB	NB

**Table 4-1: Overview of the architecture proposals for localisation and sensing (columns with the same colour rely on a similar physical deployment, while stars \* in the “Architecture” rows denote the physical entities to be located).**

## 4.2 Single-BS UE localisation with reflective RISs (C1)

### 4.2.1 Context and motivations

The most canonical way of including RIS in localisation is to consider a standard localisation scenario with one or more users and one or more BSs, with additional RIS. Communication can be in uplink or downlink. The RIS can then boost localisation performance or enable localisation when the infrastructure is not sufficient. In the former case, one can consider 4 BSs using TDoA measurements, enhanced by 1 RIS, providing an additional measurement, given that the RIS location is known. In the latter case, consider the situation with a single-antenna BS and a single antenna UE, which is insufficient for localisation. In that case, a RIS provides additional delay and AoD measurements to make the localisation possible [KKS+21b]. In the case of narrowband transmission or when the LoS path between the BS and UE is blocked, several RISs can be used to provide AoD measurements, from which the UE can be localised as the least squares intersection of lines [KDA+23].

This contribution can be seen as an extension of a study initially reported in previous deliverable D5.1 [Sec. 4.3.1, RIS5.1-22].

### 4.2.2 Overall system description

#### 4.2.2.1 Deployment scenario and physical architecture requirements

The system comprises a BS, a UE, and at least one reflective RIS. While several variations are possible in terms of physical deployment, a simple example with one single RIS and downlink pilots is considered here, for the sake of clarity.

The physical deployment and required transactions are visualized in Figure 4-1. The transactions comprise the following:



1. The UE sends an UL localisation request. This request can be complemented with coarse UE location information.
2. The BS acknowledges the request. In case the UE computes its own location, the BS also forwards its own position/orientation, as well as the position/orientation of the used RISs. The BS also sends the RIS configurations that will be used by the RIS.
3. The BS sends the relevant control data to the RIS. This control data depends on the level of autonomy of the RIS. The control data can comprise the BS location, information about the UE's approximate location, or a description of the sequence of RIS configurations that should be used.
4. The localisation process is triggered by the BS, informing the UE and the RIS.
5. The BS transmits DL pilots. These pilots are reflected by the RIS, which cycles through its assigned configurations. The UE receives and processes the DL pilots. In case the UE computes its own position, it does so at this stage.
6. In case the UE does not compute its own location information, measurements related to the received DL signals are sent to the BS. These measurements may be in the form of raw samples or measurements of angles and delays. The BS then computes the UE location.

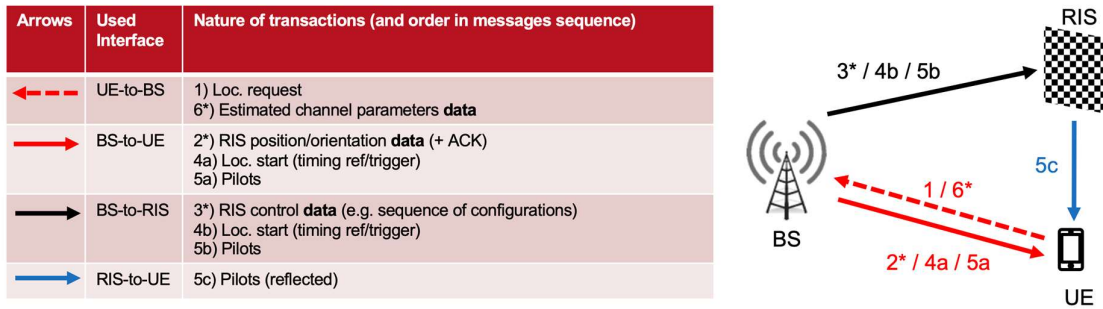


Figure 4-1: C1 - Physical deployment vs. architecture requirements, in terms of control signalling and data (\* means that data is transmitted on the over-the-air interface).

#### 4.2.2.2 Control

The RIS control (i.e., step 3 in Figure 4-1) depends on the amount of prior information the BS has regarding the UE position. There are three cases: (i) there is no information available about the UE position; (ii) the UE position is constrained to a region; (iii) the UE position is described statistically by a probability density function. These three cases are now described in more details:

- Case (i): there is **no information available about the UE position**. The options for the RIS include:
  - *Beam scanning*: In this case, the RIS is configured to illuminate a grid of discrete directions. This approach tends to be slow when the RIS is large, and beams are narrow. The number of configurations scales linearly with the number of RIS elements. In case the number of configurations is itself a constraint, the beamwidth can be broadened.
  - *Randomized beams*: In this case, the RIS is configured to illuminate a set of random directions. This approach has the risk that no beam reaches the UE with sufficient power. Even if one beam reaches the UE, this is not sufficient for estimating the AoD.
  - *Randomized RIS configurations*: In this case, each RIS element is set to a random configuration (with uniform phase) and cycles through several such configurations. In this case, the RIS configurations are not directional, and the UE coherently combines the information from different transmissions. The drawback of this option is that the UE



Document:	H2020-ICT-52/RISE-6G/D5.3		
Date:	30/06/2023	Security:	Public
Status:		Version:	1.0

needs to know the complex beam response and the exact RIS element and array response to perform coherent combining.

- Case (ii): the **UE position is constrained to a region**. The options for the RIS include:
  - *Constrained beam scanning*: This is similar to case (i), but where only beams that are directed to the region are used.
  - *Constrained randomized beam scanning*: This is similar to case (i), but where only beams that are directed to the region are used.
- Case (iii): the **UE position is described statistically** by a probability density function. The options for the RIS include:
  - *Sampling beam scanning*: This is similar to the randomized beams in case (i) and (ii), but where the directions are sampled from the density induced by the UE position density.
  - *Confidence-based beam scanning*: This is similar to constrained beam scanning in case (ii), but where the region is determined by a high-probability shape (e.g., an ellipsoid or cuboid).

#### 4.2.2.3 Signalling and data flow

The message sequence chart corresponding to the scenario from Figure 4-1 is shown in Figure 4-2.

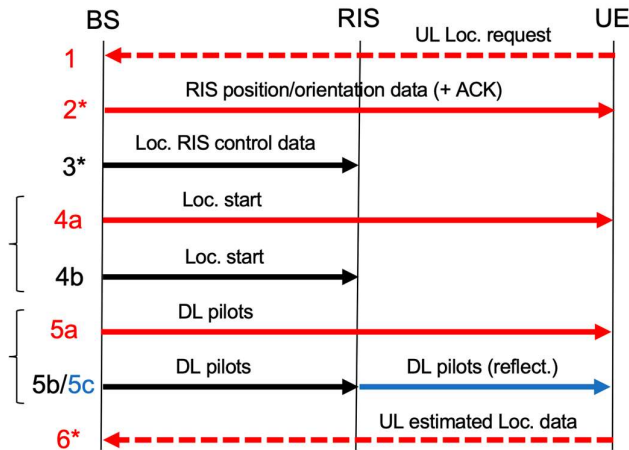


Figure 4-2: C1 - Messages sequence chart.

The time diagram corresponding to the scenario of Figure 4-1 is shown in Figure 4-3. In terms of timing, it is important to point out that in case coherent processing is used, all DL pilots (and thus also all RIS configurations) much be completed within the coherence time of the channel. However, when non-coherent processing is used, e.g., when AoDs are estimated from signal strength of beams, the time requirement is relaxed, and transmissions can occur over several coherence intervals.

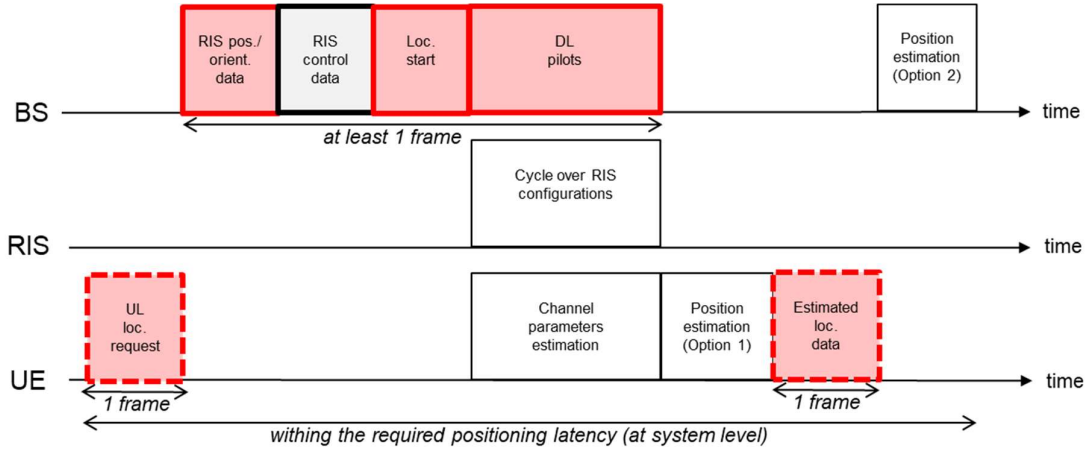


Figure 4-3: C1 - Time diagram.

### 4.2.3 Results

An example of results from [RIS5.2-22] is reviewed here, in which a single-antenna UE is to be localised with the help of a single-antenna BS and a RIS. It should be noted that without the RIS, localisation is not possible. Figure 4-4 shows the Cumulative Density Functions (CDFs) of the estimation error and the Cramer Rao Lower Bound (CRLB) of random and directional RIS phase profiles. The high mobility of the UE slightly degrades the accuracy of the velocity estimation. However, it does not affect the accuracy of the UE position estimation. The results indicate that when prior information on the UE location is available and directional beams are used (e.g., constrained randomized beam scanning from case (ii)) the localisation performance can be significantly better compared to random configurations.

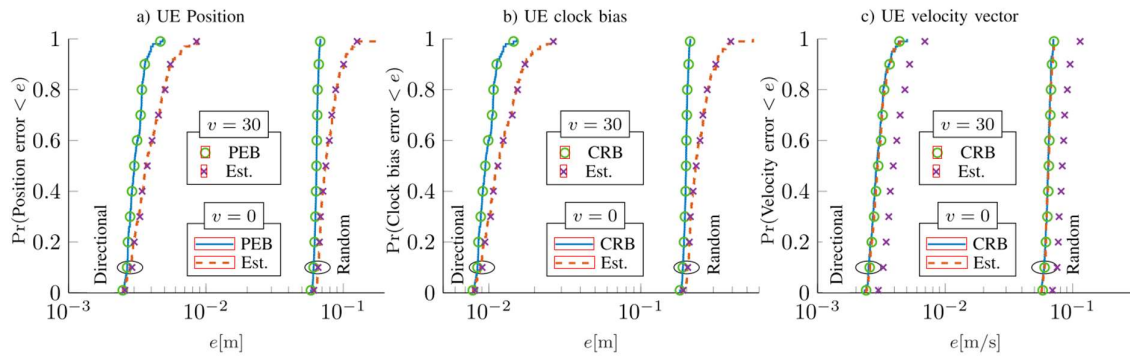


Figure 4-4: CDF of estimation error and CRLB bounds of directional and random RIS phase profiles for a) UE position, b) UE clock bias, and c) UE velocity. The UE has the position  $[-10, 10, 10]$  with the velocity  $[-v, v, 0]$ , where  $v$  is between 0 and 30 m/s.

### 4.2.4 Perspectives

This proposal can be extended in multiple ways, accounting for several RISs and several BSs, several mobile UEs, as well as a UL pilots, and location computation at the BS or at the UE side. All these variations would hence require slight variations in the control signalling. For instance, with more actors, RIS control will need to be adapted to mitigate inter-RIS interference.



---

Document:	H2020-ICT-52/RISE-6G/D5.3		
Date:	30/06/2023	Security:	Public
Status:		Version:	1.0

---

### 4.3 Passive RIS localisation with several BSs (C2)

#### 4.3.1 Context and motivations

While a RIS is generally interpreted to be part of the infrastructure, providing an additional position reference, some applications may instead focus on determining the position of the RIS itself. These applications fall in two categories:

- **RIS calibration:** when RISs are installed for supporting communication, their precise position and orientation are relatively unimportant. In contrast, for RIS-boosted or RIS-enabled positioning, the RIS position should be estimated. Since RIS installation may be prone to positioning errors, dedicated calibration methods may be employed to localise the RIS [GKC+22].
- **RIS tag localisation:** since the RIS is a low-cost, low-power device, it can be used as a smart reflective tag. To localise this tag, signals from remote transmitters that are reflected by the RIS can be received and processed by several receivers [KKD+21].

The RIS localisation problem can be solved by ToA measurements, complemented by AoA and AoD measurements (in case the transmitters and receivers have multiple antennas). By estimating the combination of AoA and AoD at the RIS, then it is possible to estimate the RIS orientation in the FF scenario.


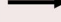

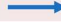

This contribution is an extension of a previous study reported in deliverable D5.1 [Sec. 4.3.6, RIS5.1-22].

#### 4.3.2 Overall system description

##### 4.3.2.1 Deployment scenario and physical architecture requirements

The system comprises a transmitting BS (TxBS), a RIS, and multiple receiving BSs (RxBS- $m$ ), where  $m$  is the BS index. One or more of the BSs may be replaced by a UE, to solve joint UE localisation and RIS localisation problems. The physical deployment and transactions are illustrated in Figure 4-5. The transactions are as follows:

1. The RIS sends a localisation request to the network, e.g., to TxBS.
2. The TxBS acknowledges the request to the RIS.
3. The TxBS instructs the RIS which RIS configurations to use, e.g., based on prior information of the RIS location, or provides the RIS with the information needed to determine its own configurations.
4. The TxBS informs the RIS and RxBSs when the localisation process will start.
5. Pilots are transmitted by the TxBS and arrive at each RxBS via a LoS path and a RIS path. During the pilot transmission time, the RIS cycles through its assigned configurations.
6. Each RxBS processes the observed signals and estimates the relevant channel parameters. These are then forwarded to a central unit, which computes the RIS location.

Arrows	Used Interface	Nature of transactions (and order in messages sequence)
	RIS-to-RxBS-m	1) Loc. request
	TxBS-to-RIS	2) ACK 3*) RIS control <b>data</b> (e.g. sequence of configurations) 4a) Loc. start (timing ref/trigger) 5a) Pilots
	TxBS-to-RxBS-m	4b) Loc. start (timing ref/trigger) 5b) Pilots
	RIS-to-RxBS-m	5c) Pilots (reflect.)
	RxBS-m-to-TxBS	6*) Estimated channel parameters <b>data</b>

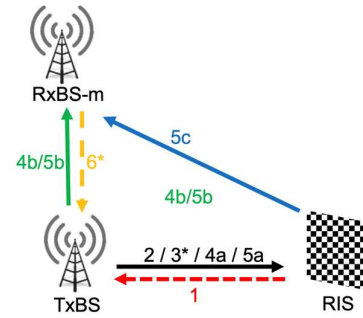


Figure 4-5: C2 - Physical deployment vs. architecture requirements, in terms of control signalling and data (\* means that data is transmitted on the over-the-air interface).

#### 4.3.2.2 Control

The RIS control depends on the prior information about the RIS location. In the absence of any such information, random RIS configurations are suitable, provided that coherent combining at the RxBSs is possible. In the presence of RIS location information, constrained (randomized) beam scanning is possible. However, in this case the beams should be generated based on a grid (samples) of the RIS location.

#### 4.3.2.3 Signalling and data flow

The message sequence chart corresponding to Figure 4-5 is shown in Figure 4-6.

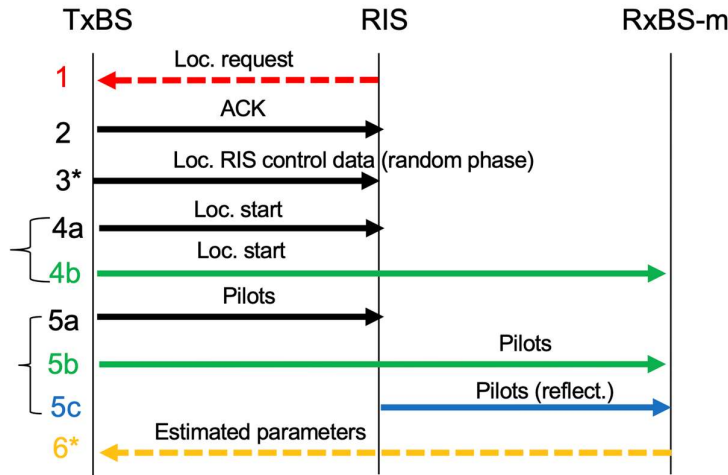


Figure 4-6: C2 - Messages sequence chart.

The time diagram corresponding to Figure 4-5 is shown in Figure 4-7. Both the message sequence chart and time diagram are similar to that of contribution C1, the only difference being that there is no UE involved.



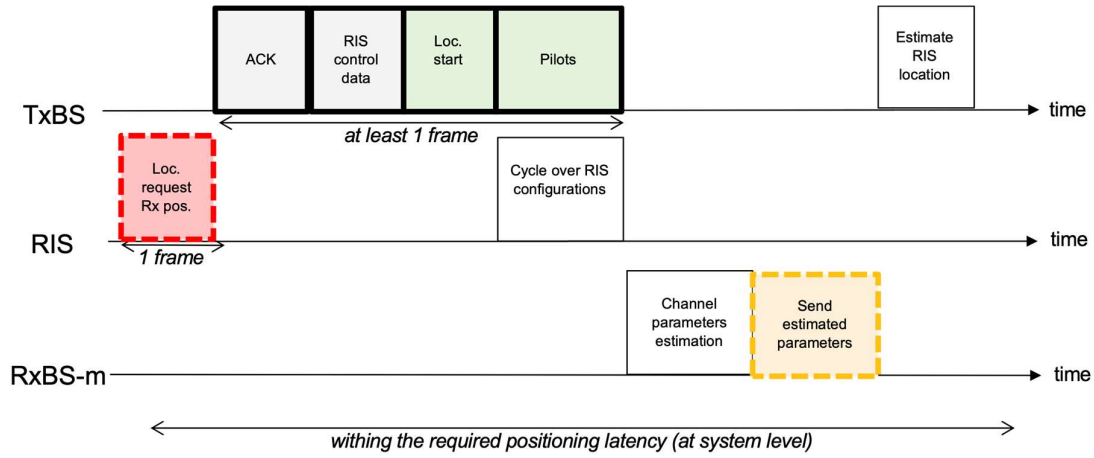


Figure 4-7: C2 - Time diagram.

### 4.3.3 Results

The performance of passive RIS localisation is shown in Figure 4-8. The position of the RIS is estimated by the ToA at multiple receivers. An example result of the PEB for the estimation of one Tx and three RxS is shown in Figure 4-8 (a). Figure 4-8 (b) shows the CDF of the PEB and the estimation error for 100 RIS configurations. It is confirmed that the proposed RIS estimator can attain the PEB as long as the PEB is less than about 8 m.

An example result of the RMSEs of the RIS position and orientation for one Tx, one Rx, and one RIS in near-field is depicted in Figure 4-9. The position and orientation of the RIS are estimated through the channel parameters (ToA, AoA at the Rx, AoD at the Tx, and AoA/AoD at the RIS for the Tx-RIS-Rx path).

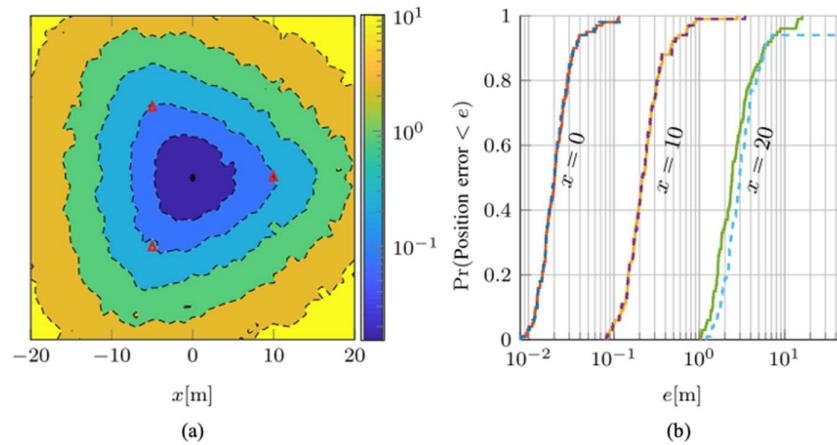
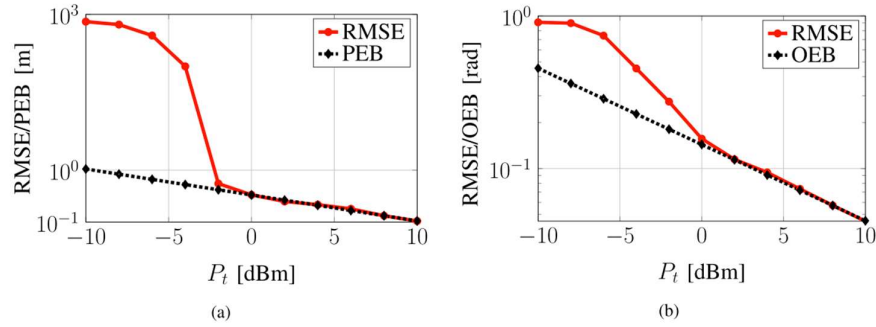


Figure 4-8: Performance of passive RIS localisation: (a) PEB of the RIS position in meters for three RXs (shown by red triangles) and one Tx (marked by black star); and (b) CDF of PEB (solid lines) and estimation error for 100 random RIS configurations.





**Figure 4-9: RMSEs and error bounds of the RIS position and orientation as a function of the transmission power, under the deployment of one Tx, one Rx, and one RIS.**

#### 4.3.4 Perspectives

The ability to estimate the combined AoA and AoD at the RIS provides the opportunity to estimate the RIS orientation. To improve performance, different RIS variants such as active RIS or hybrid RIS may be considered.

### 4.4 BS-free UE localisation and environment mapping with one reflective RIS (C3)

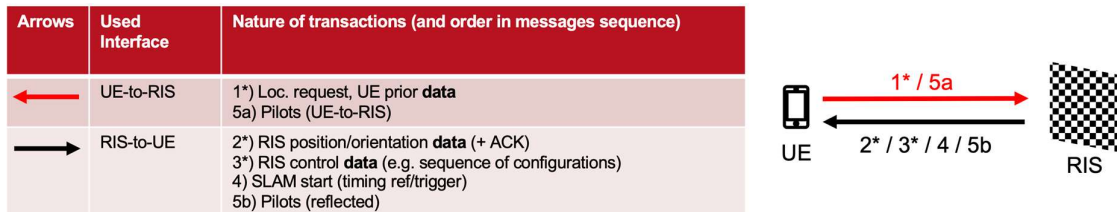
#### 4.4.1 Context and motivations

The aim of this contribution is to adaptively design the RIS phase profiles given the prior UE location information, effectively illuminating the UE from the RIS, which in turn improves the Simultaneous Localisation And Mapping (SLAM) performance. This scenario considers wireless signal propagation environments, where there is no BS, and the propagation environment comprises a full-duplex UE, a RIS, and multiple landmarks [KCK+22]. The full-duplex UE is moving and periodically transmits signals (preferably at mmWave frequencies to benefit from “geometric” channel behaviour, sparser multipath and spatial filtering, which are all beneficial to localisation and sensing), from which the following multipath components are generated by the propagation environment: i) UE-RIS-UE, resulting in the phase-shifted signals at the RIS by the designed RIS phase profiles; ii) UE-landmarks-UE, generated by the reflection or scatter at the landmarks. Then, the UE receives the back-propagated signals consisting of single-bounce signal propagation, due to the highly attenuated power of multiple-bounce signals. Then, the UE estimates its state (position, heading, speed), as well as positions of landmarks [KCK+22]. Here, the contributions are to exploit the NLoS paths for mapping and design the temporal-spatial RIS profiles.

This work is an extension of one contribution already introduced in D5.3 [Sec. 4.3.2, RIS5.1-22].

#### 4.4.2 Overall system description

##### 4.4.2.1 Deployment scenario and physical architecture requirements



**Figure 4-10: C3 - Physical deployment vs. architecture requirements, in terms of control signalling and data (\* means that data is transmitted on the over-the-air interface).**

The system consists of a full-duplex UE and a reflective RIS, where the RIS is attached to large surfaces such as buildings or walls. Again, while various physical deployment configurations are possible, a simple example involving a single RIS and a UE is considered, for the sake of clarity and simplicity.

The physical deployment and transactions are illustrated in Figure 4-10, and the transactions are as follows:

1. The UE sends a localisation request and forwards the UE prior data.
2. The RIS acknowledges the request and forwards the RIS position/orientation information to the UE.
3. The RIS computes the RIS configurations and forwards the relevant control data to the UE.
4. The localisation process is triggered by the UE, informing the RIS.
5. The UE transmits the pilots. The impinging pilots to the RIS are reflected by the designed RIS configurations (in step 3), and the pilots are reflected or scattered by other landmarks. The UE receives either reflected or scattered signals, and then estimates the UE state and the positions of landmarks.

#### 4.4.2.2 Control

The RIS control depends on the prior information of the UE location. In the absence of such information, random RIS configurations are suitable. In the presence of RIS location information with a probability density function, the method of confidence-based beam scanning is available as follows. The spatio-temporal RIS phase profile is designed, to adaptively illuminate the UE position uncertainty. First, the RIS phase profile is designed to be balanced in the time domain by adopting a temporal coding approach [KSA+22] to separate the RIS-induced path from multipath. Due to a large number of RIS elements, the RIS directional phase may not adequately cover the UE position uncertainty. To uniformly illuminate the UE position uncertainty, the spatial domain is considered in the RIS phase profile design, as shown in Figure 4-11. The UE uncertainty region is divided into multiple grids, and each grid is covered by a transmission. For each transmission, the phase of each RIS element is configured to one specific point on the grid.

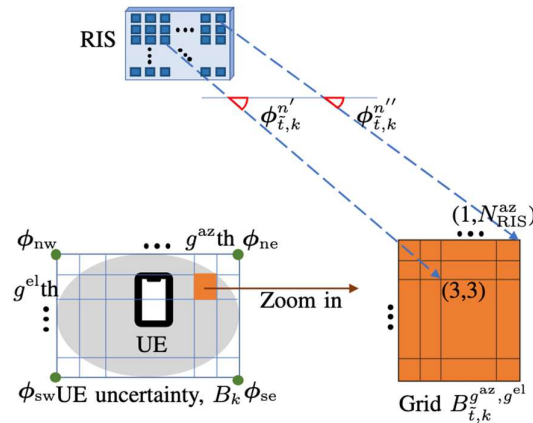
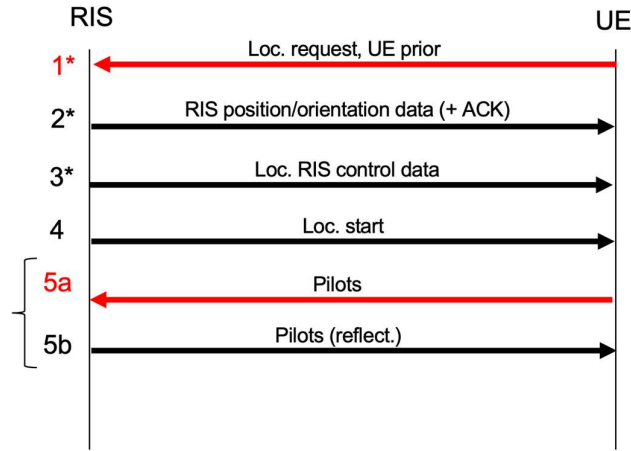


Figure 4-11: C3 - RIS phase profile for multiple spatially-uniform beams.

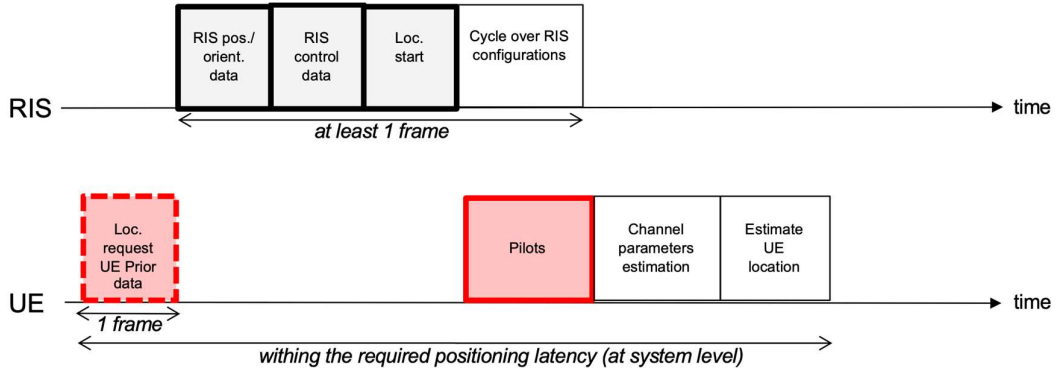
#### 4.4.2.3 Signalling and data flow

The messages sequence chart corresponding to the scenario of Figure 4-10 is shown in Figure 4-12.



**Figure 4-12: C3 - Messages sequence chart.**

The time diagram corresponding to the scenario of Figure 4-10 is shown in Figure 4-13. Both the messages sequence chart and the time diagram are similar to that of contribution C1, and the only difference is that there is no BS involved.

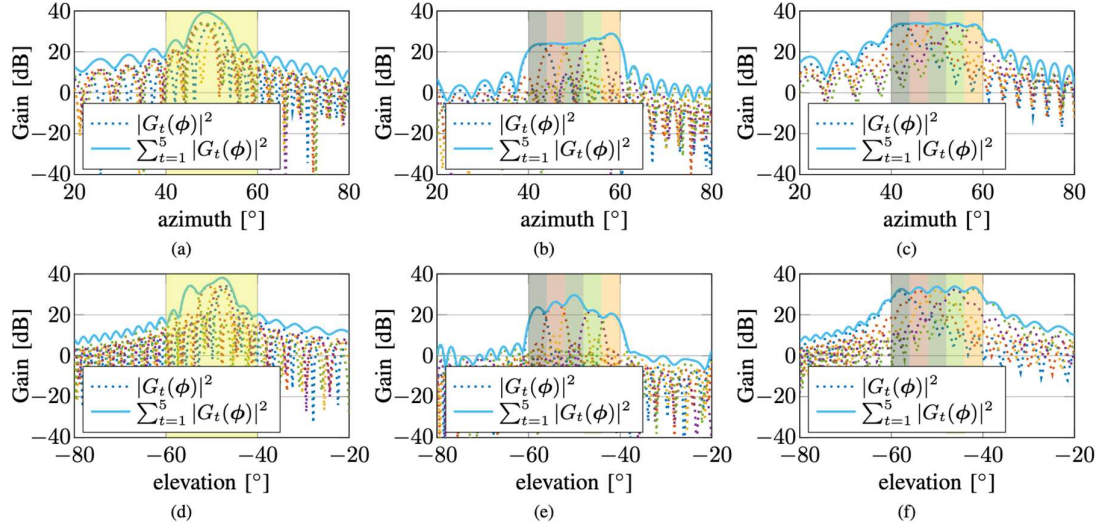


**Figure 4-13: C3 - Time diagram.**

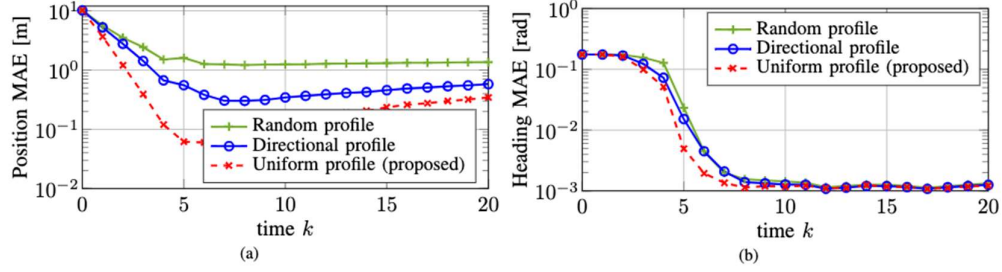
#### 4.4.3 Results

The results of this work are as follows. The proposed RIS phase profile outperforms directional and random reflective beams, in terms of the RIS-based power gain for wireless communication. This happens because the proposed RIS phase profile can uniformly illuminate the UE position uncertainty. Figure 4-14 shows that the entire angular sector determined by the UE position uncertainty can be illuminated by the proposed phase profiles with sufficient power, whereas the directional phases cannot uniformly illuminate the desired angular sector, and thus, the UE cannot be provided with sufficient reflected power from the RIS to ensure good positioning performance.

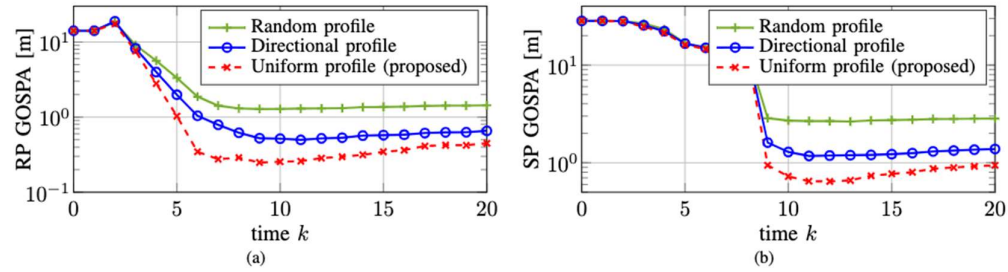
With the proposed RIS phase profile, a significant SLAM performance gain can be obtained, compared to that with random and directional phase profiles, as shown in Figure 4-15 and Figure 4-16.



**Figure 4-14: Beam patterns of the 2D RIS in the azimuth (a)-(c) and elevation (d)-(f) domains: (a) and (d) with directional phases; (b) and (e) with optimised phases; (c) and (f) with the proposed uniform phases.**



**Figure 4-15: Localisation performance over time steps: Mean Absolute Errors (MAEs) of (a) position and (b) heading estimates.**



**Figure 4-16: Mapping performance over time steps: (a) reflection point and (b) scattering point.**

#### 4.4.4 Perspectives

This contribution can be extended towards a multi-RIS and/or multi-UE scenario, which would require slightly different RIS control and signalling, as well as inter-RIS coordination (typically, with dedicated transmission scheduling methods among the UEs).



## 4.5 BS-free cooperative UE localisation through sidelinks with one reflective RIS (C4)

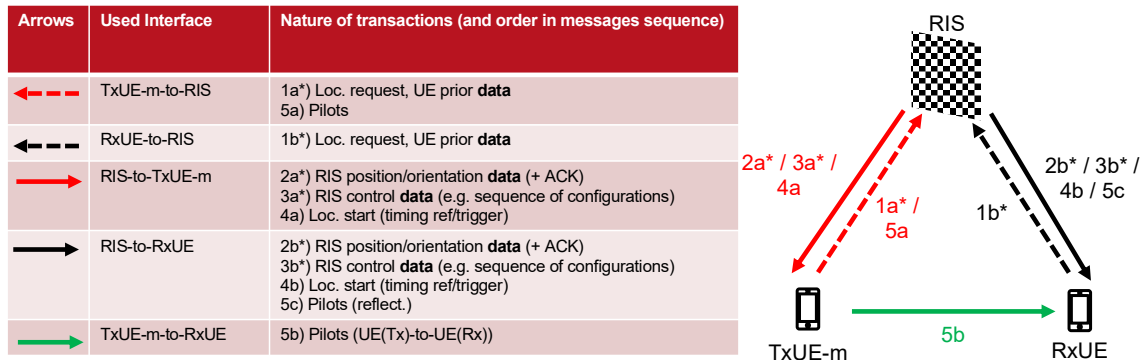
### 4.5.1 Context and motivations

The aim of this contribution is to control the RIS phase profiles and to estimate the locations of several UEs via sideline transmissions. This scenario considers wireless signal propagation environments, where there is no BS, and the propagation environment comprises UEs and a RIS [CKA+23]. The UEs TxUEs transmit signals (e.g., preferably at mmWave frequencies for the same reasons as in proposal C3, without loss of generality though). The transmitted signals are propagated in the environment, and the RxUE receives the following multipath: i) TxUEs-RIS-RxUE, resulting in the phase-shifted signals at the RIS by the designed RIS phase profiles; ii) TxUEs-RxUE. The RxUE localisation problem can then be solved by the channel parameters (such as ToA, AoA, AoD) for multiple RIS paths.

This work is a new contribution, compared to the previous deliverable D5.1.

### 4.5.2 Overall system description

#### 4.5.2.1 Deployment scenario and physical architecture requirements



**Figure 4-17: C4 - Physical deployment vs. architecture requirements, in terms of control signalling and data (\* means that data is transmitted on the over-the-air interface).**

The system consists of the multiple transmitting UEs (TxUEs- $m$ , where  $m$  is the UE index), a RxUE, and a reflective RIS.

The physical deployment and transactions are illustrated in Figure 4-17, and the transactions comprise the following steps:

1. The TxUEs and RxUE send localisation requests to the network and forward the UE prior data.
2. The RIS acknowledges the request and forwards its position/orientation data to the UEs.
3. The RIS computes the RIS configurations and forwards the relevant control data to the TxUEs and RxUEs.
4. The localisation process is triggered by the UEs, informing the RIS.
5. The TxUEs transmit the pilots. The impinging pilots to the RIS are reflected by the designed RIS configurations (in step 3), and the RxUE receives the tuples of LoS and NLoS paths for the different TxUEs. Then, the RxUE estimates channel parameters and its location.

#### 4.5.2.2 Control

The RIS control depends on prior information on the TxUEs and RxUE. In the absence of any prior information, random RIS configurations are adequate. In the presence of prior information with a probability density function, the method of confidence-based beam scanning is available. Due to the different TxUEs, the RIS control can be designed while considering a temporal RIS phase coding or even sub-RISs.



#### 4.5.2.3 Signalling and data flow

The messages sequence chart corresponding to Figure 4-17 is shown in Figure 4-18.

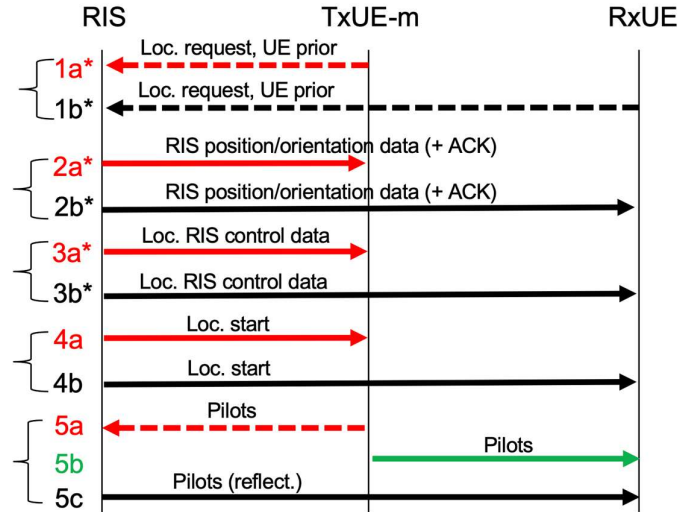


Figure 4-18: C4 - Messages sequence chart.

The time diagram corresponding to Figure 4-17 is shown in Figure 4-19. Both the messages sequence chart and the time diagram are similar to that of contribution C1, the only difference being that multiple TxUEs are involved instead of a BS.

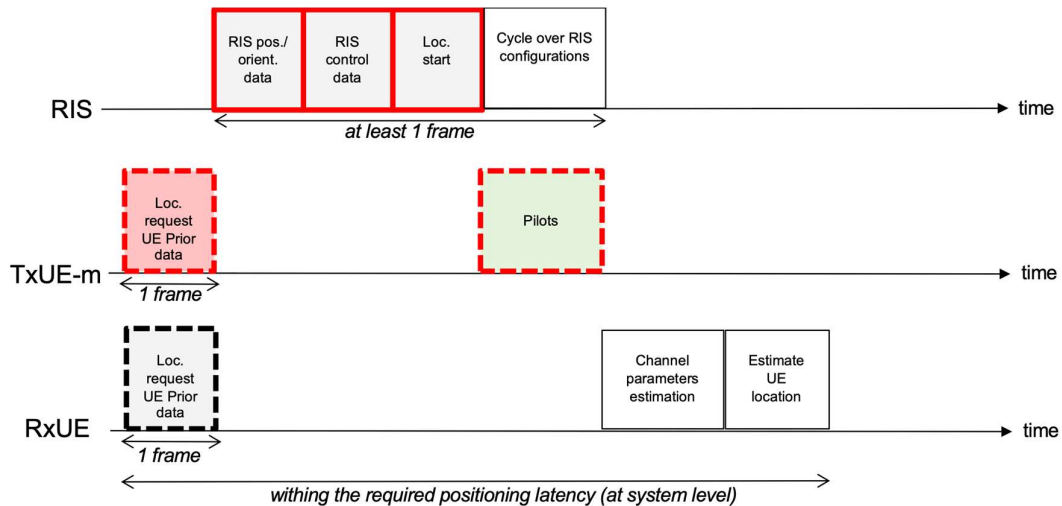


Figure 4-19: C4 - Time diagram.

#### 4.5.3 Results

In the chosen illustration scenario, three UEs and one RIS are deployed, and the RIS phase profiles are random. Figure 4-20 shows the PEBs of RIS-enabled cooperative UE localisation for different sizes of RIS elements. As the number of RIS elements increases, the PEBs have a performance gain.



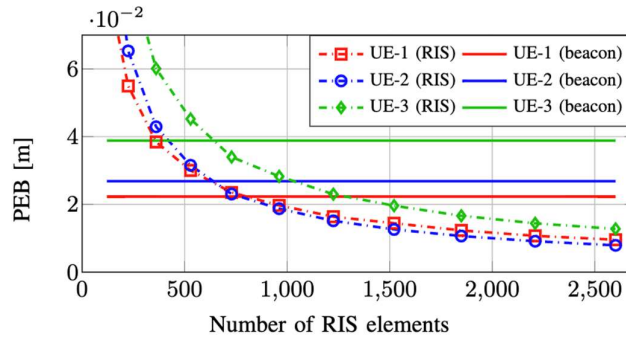


Figure 4-20: PEBs of RIS-enabled cooperative UE localisation for different sizes of RIS (in terms of the number of elements).

#### 4.5.4 Perspectives

The perspectives of this contribution relate to the extension towards several RISs, which cooperate to position the UEs via sidelink transmissions.

### 4.6 Single-BS UE localisation with one reflective RIS in near field (C5)

#### 4.6.1 Context and motivations

This research concerns the design and implementation of various RIS profile control mechanisms in light of the harsh imposed scenarios where the BS-UE direct path is blocked. Three different RIS profiles are implemented, random, directional, and a new proposed localisation-optimal design suitable to NF regime, which relies on minimising the PEB. In RIS-assisted wireless systems, especially if localisation-oriented, the optimisation of the reflection profile is a major challenge when operating in reflective mode, especially in uncontrolled reflection amplitude scenarios. While conventional solutions for RIS-aided communications focus on enhancing SINR at UE through cascade channel estimation or prior UE location information, the overall localisation strategy must consider RIS beam pattern design from a precoding standpoint. Moreover, in harsh blocked environments, the RIS serves as a localisation enabler where its reflections are meant to compensate for the loss of the direct path relying on the curved nature of the wavefront in NF regime. We thus propose a new location-optimal phase profile design for the reflective RISs, which is based on minimising the downlink (DL) positioning performance bound, so-called PEB, in NLoS conditions. It relies on previous studies on far-field (FF) LoS DL localisation SISO MC transmissions in reflection mode [KKS+21b], as well as on NF localisation in receiving mode [GD21], [AKK+21].

This contribution, which was already reported to a large extent in deliverable D5.1 [Sec. 5.2.5, RIS5.1-22], is subject to two paper publications [RDK+21] and [RDK+22a].

#### 4.6.2 Overall system description

##### 4.6.2.1 Deployment scenario and physical architecture requirements

The proposed physical architecture, which is shown in Figure 4-22, consists of the following entities:

1. One single-antenna BS acting as a transmitter.
2. One single-antenna UE acting as a receiver and performing the localisation process and transmitting this information back to the BS (or alternatively, transmitting the required radio metrics extracted out of received signals back to BS for the calculation of UE location).
3. One planar R-RIS with various sizes (i.e., number of elements), mounted on big surfaces like walls.

From a logical architecture standpoint, a RISC element (likely collocated with the BS, but not necessarily) is in charge of deciding which RIS phase configurations shall be applied by the RISA, given the assumed prior UE location knowledge.

This system setup is assumed to be in a 3D indoor environment operating at relatively short distances (especially the distance from RIS to UE) with obstacles blocking the direct BS-UE path, as depicted in Figure 4-21. The final position estimation can be performed either on the UE's side or in a distant centralized server, provided that the measured radio metrics are transmitted from the former.

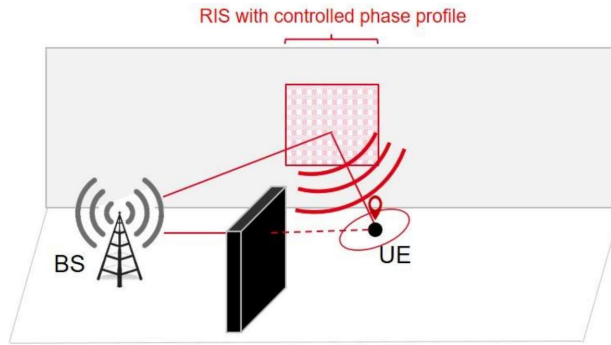




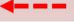



Figure 4-21: Canonical scenario considering optimising reflective RIS profiles in NLOS SISO DL positioning.

Arrows	Used Interface	Nature of transactions (and order in messages sequence)
	UE-RIS	1a) UL Loc. request 5a*) UL estimated Loc. <b>data</b> (e.g., channel parameters or position...)
	RIS-BS	1b) Reflection of Loc. request 5b*) UL estimated Loc. <b>data</b> (e.g., channel parameters or position...)
	BS-to-RIS	2*) RIS control <b>data</b> (e.g. sequence of configurations) 3) Loc. start (timing ref/trigger) 4a) DL pilots
	RIS-to-UE	4b) DL pilots (reflected)
	UE-to-BS	Blocked by obstacle
	BS-to-UE	Blocked by obstacle

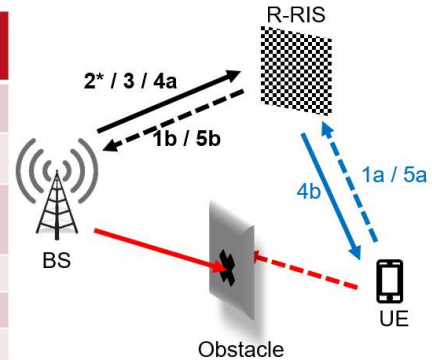


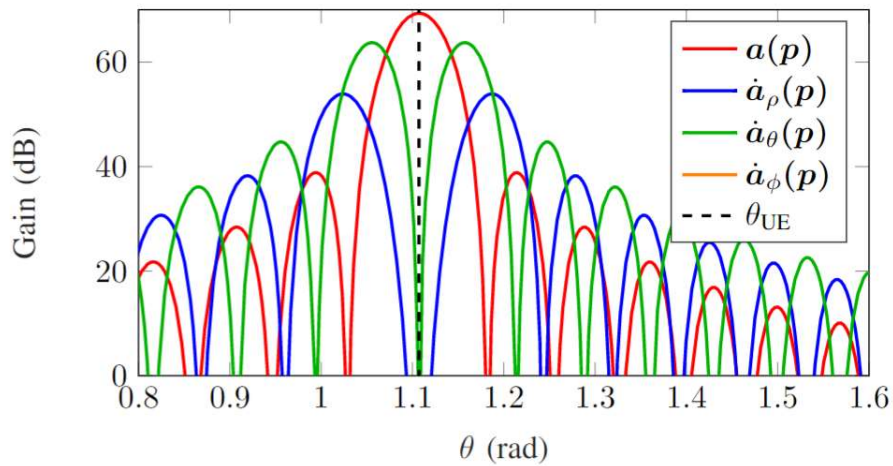
Figure 4-22: C5 - Physical deployment vs. architecture requirements, in terms of control signalling and data (\* means that data is transmitted on the over-the-air interface).

#### 4.6.2.2 Control

In the proposed scheme, in case of steady-state NLoS regime (i.e., prior to initiating the localisation procedure), an UL communication link between the UE and the BS should be pre-established through the RIS so as to forward the UL request. In this case, classical directional beams shall for instance be applied at the RIS to ensure sufficiently high SNR at the receiving BS, given that the relative positions of both



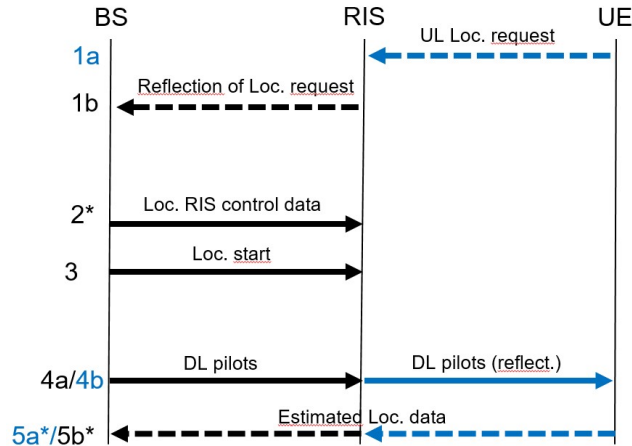
the BS and the RIS are known and static. Subsequently, for the localisation procedure itself, a new RIS phase profile is applied, while relying on the minimization of the theoretical CRLB on position estimation (i.e., the PEB) and assuming the UE position to be known a priori. For this sake, the considered SISO DL transmission model includes a generic RIS response model encompassing both NF and FF regimes. Instead of optimising the element-wise reflection coefficients of the RIS, which is a hefty task, another approach is considered where four distinct optimal beams (directional and its derivatives w.r.t. the spherical spatial dimensions, see Figure 4-23) are applied for NF localisation and their relative weights are then optimised to get the minimal error bounds possible, given the latest known UE position. The performance of this location-optimal reflection profile design is then compared with another two benchmark designs, namely the random and directional phase profile design.



**Figure 4-23: Illustration of orthonormalized beams, i.e., the steering beam (red), and its three derivatives w.r.t. spherical coordinates (respectively in blue, green, and orange), suitable to RIS-aided NF NLoS localisation.**

#### 4.6.2.3 Signalling and data flow

The messages sequence chart associated with Figure 4-22 is shown in Figure 4-24, while Figure 4-25 represents the corresponding time diagram.



**Figure 4-24: C5 - Messages sequence chart.**

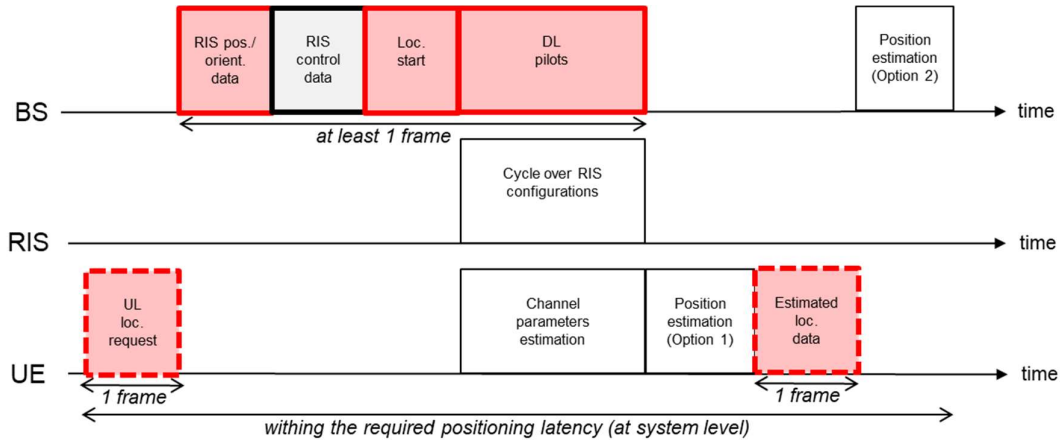


Figure 4-25: C5- Time diagram.

#### 4.6.3 Results

First, simulations are carried out with random profiles applied to the Reflective RIS (R-RIS) [RDK+21] in a canonical SISO DL MC scenario. We then show the benefits of incorporating a single RIS operating in NF to enable localisation continuity. Accordingly, whenever the UE is close enough to the RIS and/or when the RIS is large enough, exploiting the reflected signal wavefront's curvature in NF could be sufficient to directly infer UE's position in the absence of the direct path, even if the achievable accuracy remains relatively low (see Figure 4-26).

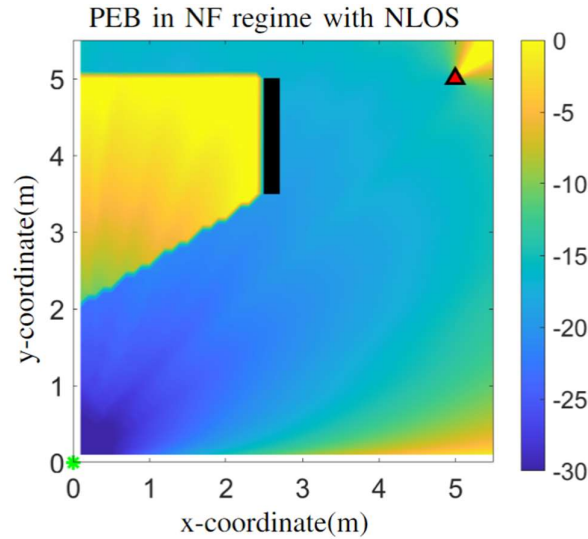
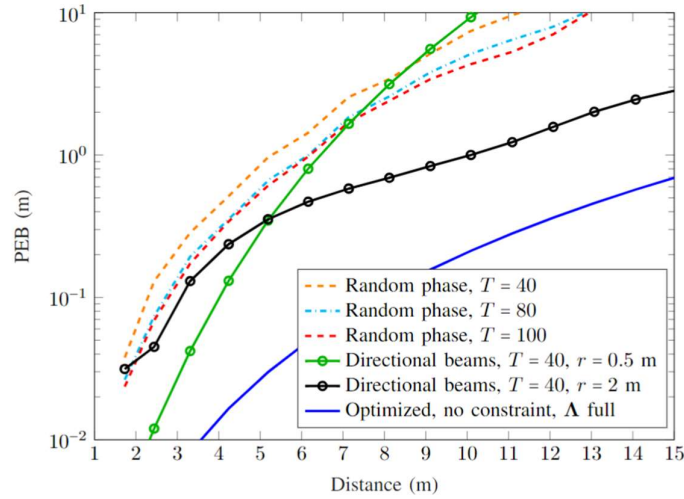


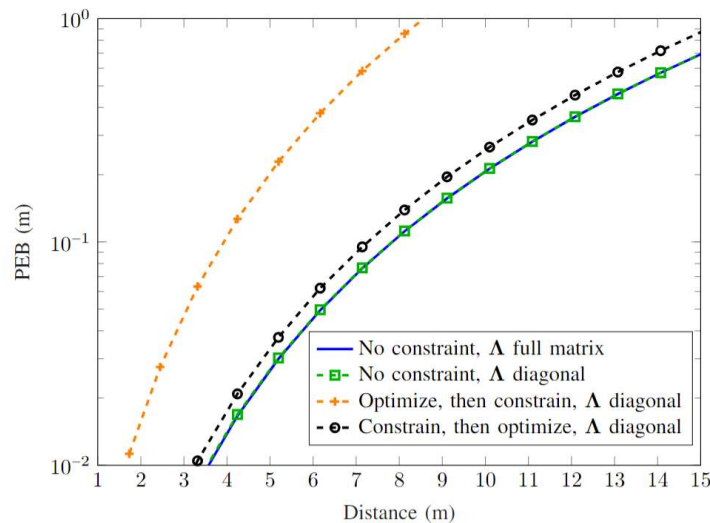
Figure 4-26: PEB heatmap (in dB), as a function of UE location ( $z = 0$ ) for a generic RIS response model (supporting NF), with one planar reflective RIS of  $32 \times 32$  elements in  $[0, 0, 0]$ m, one BS in  $[5, 5, 0]$ m and a finite obstacle parallel to the  $y$  axis (black).

Addressing this issue of limited accuracy in NLoS positioning, other numerical simulations carried out in a canonical SISO DL scenario [RDK+22a] confirm that the proposed optimized RIS profile, involving a combination of four beams (the steering vector and its derivatives) at the RIS with weights determined

through a PEB minimisation procedure, outperforms traditional random and directional beam codebook designs, as illustrated in Figure 4-27. Beyond, to ensure a realistic passive behaviour of the RIS, the desired beams must be constrained onto the unit circle. The order of the "constraining" and "optimising" procedures is absolutely crucial. Figure 4-28 shows that utilising unconstrained beams yields the best results, as expected, while the "optimise then constrain" strategy leads to the worst performance and the "constrain then optimise" strategy approach lies in between, at a level fairly close to the unconstrained beam performance.



**Figure 4-27: PEB comparison as a function for the UE-RIS distance, with the proposed optimised RIS profile, conventional directional and random codebook designs, for different numbers of transmissions  $T$  and different prior UE position uncertainty (for the directional design only).**



**Figure 4-28: PEB as a function of the UE-RIS distance for different variants of the problem solver (incl. the "unconstrained", "optimise then constrain" and "constrain then optimise" schemes regarding RIS beams generation).**

#### 4.6.4 Perspectives

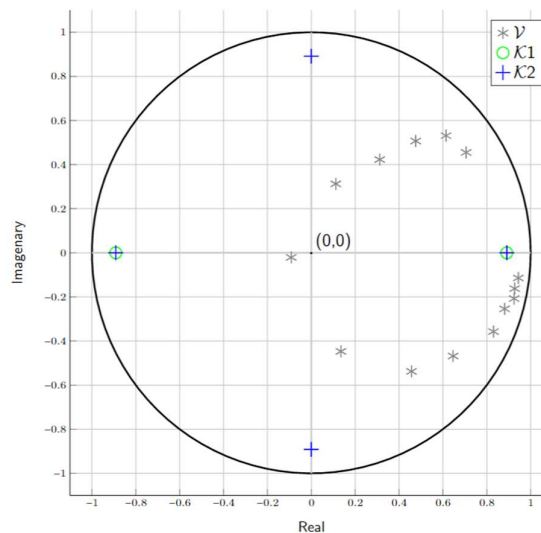
Given that the system prompts RIS profile optimisation with prior knowledge of the UE position, a natural progression of this study concerns the incorporation of position uncertainty into the optimisation process (as part of the prior knowledge). This could also be the case in dynamic scenarios with mobile UEs, leveraging for instance the output of a tracking filter.

### 4.7 Single-BS UE localisation with one reflective RIS in near field under real hardware constraints (C6)

#### 4.7.1 Context and motivations

In the physical realm, suffering from imperfections and impairments is indeed common for cheap and low-complexity hardware devices like the ones that make up the passive RIS. Accordingly, after theoretically designing the optimal R-RIS phase profiles for NF NLoS DL positioning through unconstrained PEB minimisation, the practicability of the solution must be studied, while accounting for the specificities of realistic hardware prototypes. More specifically, we considered the feasibility of approximating complex RIS beam patterns (e.g., the steering one and its derivatives) from a pre-defined look-up table that characterizes the distribution of RIS element-wise complex reflection coefficients for a given real prototype (see Figure 4-29). One first objective of this study was hence to evaluate the actual positioning performance that could be achievable with several real RIS hardware prototypes/designs while applying the initial PEB-based RIS phase control scheme. Another objective was to present a practical optimisation framework that could approximate arbitrary beam patterns (and typically, that required by the proposed PEB-based RIS control scheme), directly based on such look-up tables. Specifically, two reflect-arrays developed and characterized in the context of RISE-6G WP3 were considered in the study. The proposed low-complexity optimisation framework is hence shown to properly generate the steering and derivative beam patterns required for positioning, with reasonable loss in terms of both beam pattern fidelity and positioning performance.

This contribution, which is an extension of a previous study reported in deliverable D5.1 [Sec. 5.2.6, RIS5.1-22], has been subject to two paper publications [RDK+22b] and [RDK+23].



**Figure 4-29: Distribution of RIS element-wise complex reflection coefficients in the complex plane, according to the lookup tables of 3 real R-RIS prototypes designed in RISE-6G.**

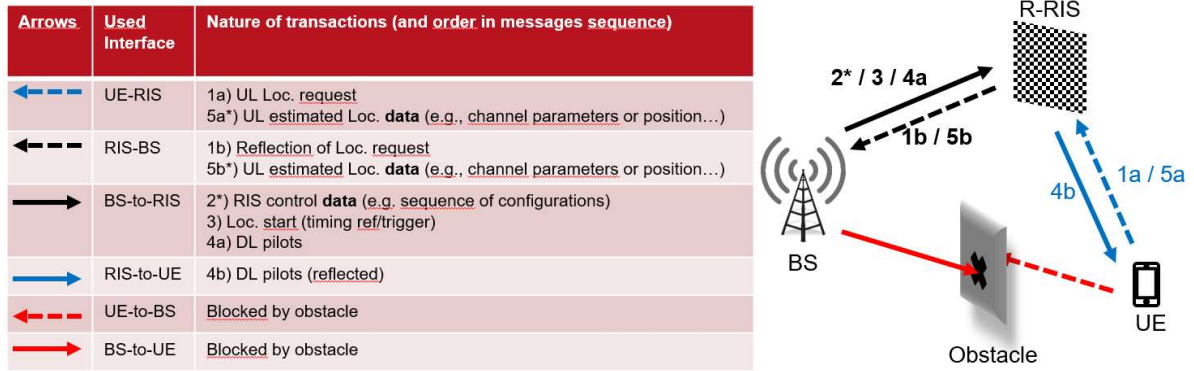
## 4.7.2 Overall system description

### 4.7.2.1 Deployment scenario and physical architecture requirements

Like in the previous contribution C5, the physical architecture shown in Figure 4-30 consists of:

1. One transmitting BS with a single-antenna.
2. One single-antenna receiving UE performing the localisation process and transmitting this information back to the BS.
3. A planar R-RIS with various sizes.

In this case again, from a logical architecture standpoint, a RISC element (likely co-located with the BS, but not necessarily) is in charge of deciding which RIS phase configurations shall be applied by the RISA, given the assumed prior UE location knowledge.



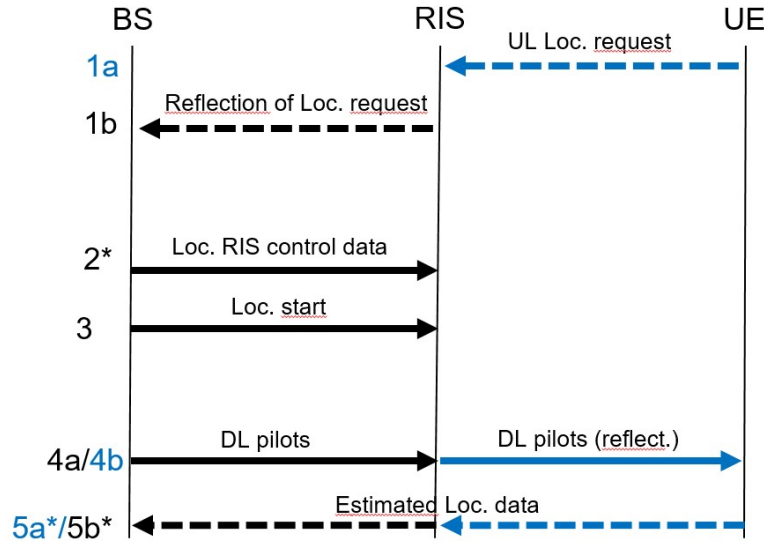
**Figure 4-30: C6 - Physical deployment vs. architecture requirements, in terms of control signalling and data.**

### 4.7.2.2 Control

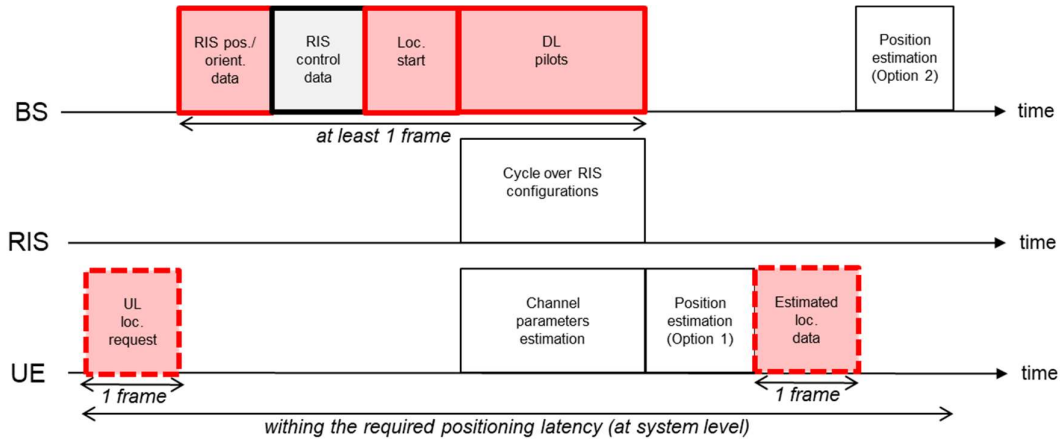
As in subsection 4.6.2.2, the newly devised RIS phase profile control mechanism is utilised herein. The applied RIS element-wise reflection coefficients are thus determined by optimising the weights of the previously mentioned four beams, while still relying on the PEB metrics. To do so, an efficient numerical method is put forward, where the desired beams are first defined onto discretised domains and then accordingly, the initial optimisation problem is stated as a RIS beam pattern synthesis problem for which a dedicated optimising routine is developed. The latter determines the optimal RIS phase profile to be applied (i.e., the best assignment of addressable reflection coefficients per RIS element) that best matches the desired beam patterns. To deal with this optimisation problem, a simple projected gradient descent algorithm is used. To further simplify our method, and avoid any tremendous computational costs, the beams are then re-expressed in terms of the spherical coordinates and the optimisation objective is redefined accordingly.

### 4.7.2.3 Signalling and data flow

The messages sequence chart associated with Figure 4-30 is identical to Figure 4-24, as shown in Figure 4-31, while Figure 4-32 represents the corresponding time diagram, which is also similar to Figure 4-25.



**Figure 4-31: C6 - Messages sequence chart.**

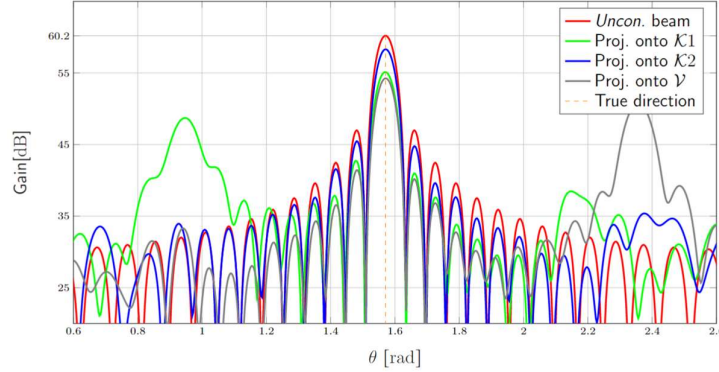


**Figure 4-32: C6 - Time diagram.**

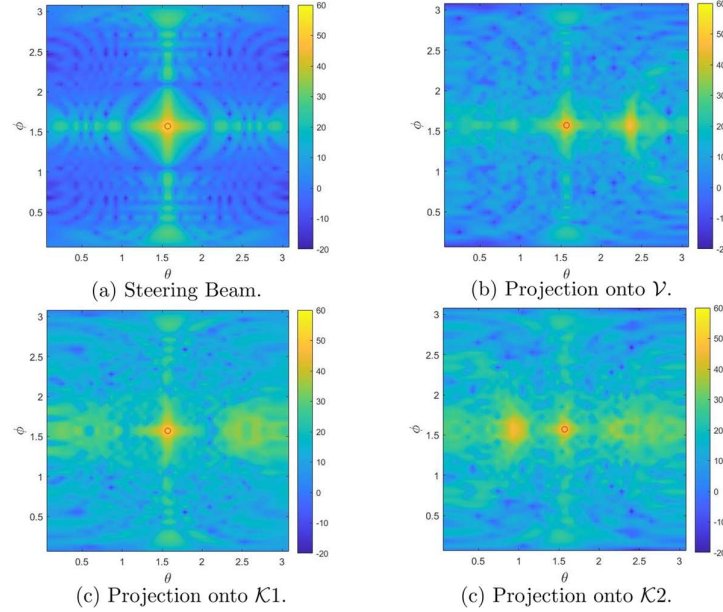
### 4.7.3 Results

In order to evaluate the efficiency of the proposed low-complexity beam synthesis method, we first analysed the distribution of the addressable reflection coefficients per RIS element in the complex plane for different hardware prototypes (as per the characterized lookup tables) and how this distribution could impact the fidelity of the generated RIS beams (with respect to the desired ones). As an example, we present the 1D and 2D beam representations of both ideal and approximated directional RIS beams in Figure 4-33 and Figure 4-34, respectively. We then observe a degradation of the maximum value in the main lobe of the beam in the 1D representation, as well as the presence of sidelobes. This behaviour is also observed in the 2D representation, where multiple peaks appear alongside the intended one.





**Figure 4-33: Examples of steering beam gains (unconstrained and approximated under RIS hardware constraints) in 1D, as a function of the azimuth angles, while accounting for the RIS element responses of real hardware prototypes through look-up tables.**



**Figure 4-34: Examples of steering beam gains (unconstrained and approximated under RIS hardware constraints) in 2D, as a function of both azimuth and elevation angles, while accounting for the RIS element responses of real hardware prototypes through look-up tables.**

Furthermore, beyond beam fidelity considerations, we have also extended the assessment of our RIS beam approximation method for different prototypes via PEB evaluations, evaluating the best achievable localisation performance versus both RIS-UE distance and RIS-UE azimuth angle, as shown in Figure 4-35 and Figure 4-36 respectively. Some general trends, regarding different RIS phase designs and distinct RIS prototypes, are thus common in both figures. First, comparing the RIS profile designs, we see as expected that the location-optimal RIS phase design still outperforms directional and random ones, despite the beams approximation procedure, and second, that the ability to approximate the arbitrary beams, more specifically, to direct the power of the main lobe towards the desired direction has a positive impact on the performance bound level. This confirms that the final achievable localisation performance is quite strongly correlated to the quality of the approximation of the needed beams under imposed hardware constraints.



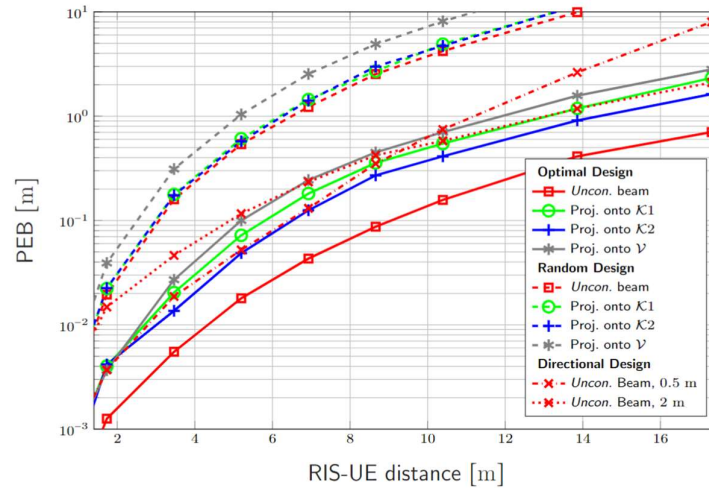


Figure 4-35: PEB as a function of RIS-UE distance for ideal and generated localisation-optimal RIS beams, as constrained by the real look-up tables of various characterized hardware prototypes.

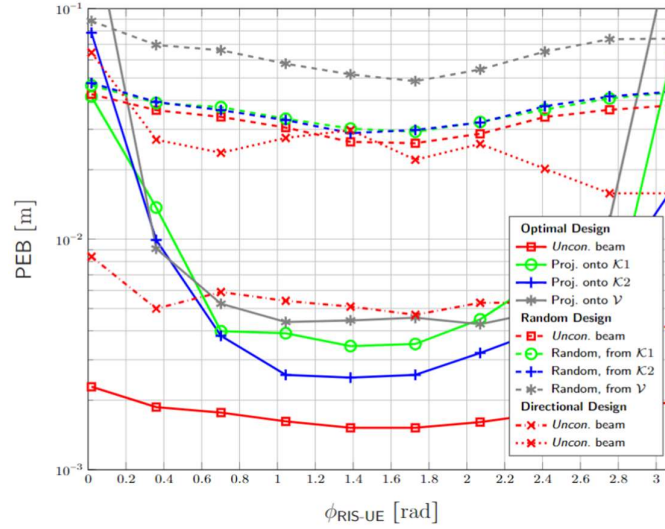


Figure 4-36: PEB as a function of RIS-UE azimuth angle for ideal and generated localisation-optimal RIS beams, as constrained by the real look-up tables of various characterized hardware prototypes.

#### 4.7.4 Perspectives

Future works should investigate the conjugated effects of both the RIS beam approximation method and the distribution of RIS element-wise complex reflection coefficients on the performance of real estimation algorithms (i.e., rather than just assessing theoretical bounds).

### 4.8 BS-free UE localisation with several sensing RISs (C7)

#### 4.8.1 Context and motivations

Building on the idea of Contribution C4, another system for localising users without the presence of a BS is proposed. The main difference in this architecture is the fact that multiple RISs are assumed to be

placed around the target area. Each RIS is equipped with a RX Radio Frequency (RF) chain, which greatly reduces the energy consumption of the receiving surfaces.

This contribution, which was already reported to a large extent in deliverable D5.1 [Sec. 4.3.5, RIS5.1-22], is subject to one paper publication [AVW22].

## 4.8.2 Overall system description

### 4.8.2.1 Deployment scenario and physical architecture requirements

The architecture consists of one static UE multiple receiving RISs (each equipped with a single RX-RF chain attached to all the RIS elements), and one central orchestrator, as depicted in Figure 4-37. In an indoor 3D environment with multipath, operating in the mmWave frequencies (for the same reasons as in proposal C3, without loss of generality though) under the far-field assumption, AoA estimations for each RIS are being performed and combined at the central controller for the UE to be localised.

Note that in this specific case with no BS but multiple RISs, a so-called RISO is abusively represented in Figure 4-37 as part of the physical architecture (although it would formally take part in the architecture, as a logical block), just to materialize the fact that, beyond logical architecture considerations, a tier physical entity on the infrastructure side would still be in charge of interacting with the multiple RIS to coordinate them.

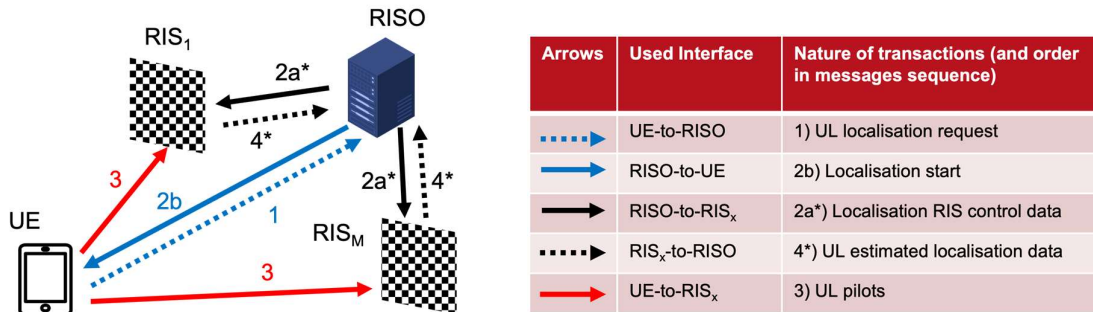


Figure 4-37: C7 - Physical deployment vs. architecture requirements, in terms of control signalling and data (\* means that data is transmitted on the over-the-air interface).

### 4.8.2.2 Control

The localisation is performed as follows and the corresponding sequence of messages is depicted in Figure 4-38:

1. The procedure is initiated by the UE and coordinated by the AMF/Location Management Function (LMF) and RISO. The UE transmits a localisation request signal.
2. The RISO responds with an ACK that signifies that the localisation procedure is starting. The same message is transmitted via the over-the-air interface to all M RISs.
3. Each RIS receives the impinging signal from the UE with a predefined RIS element configuration (determined by the RISC) and stores it at the central controller. This step is repeated each time with a different RIS element configuration (determined by the RISC) until a predefined number of signal measurements are gathered at the central controller, for each RIS.
4. The central controller performs an AoA estimation for each RIS. The estimations are transmitted to the central RISO, which fuses the AoA estimations to localise the UE.

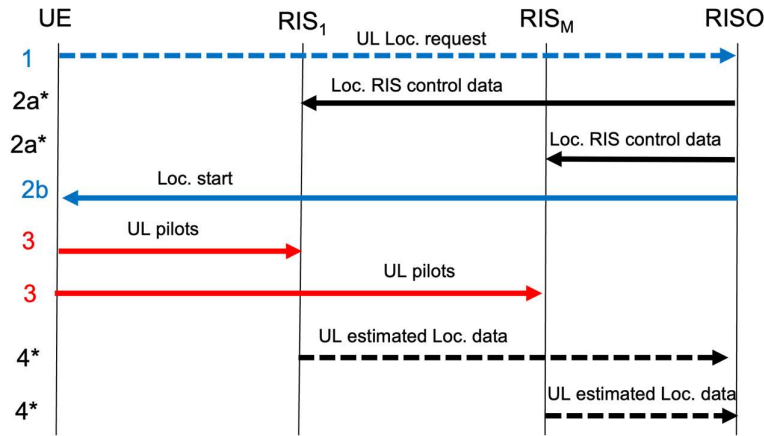


Figure 4-38: C7 - Messages sequence chart.

#### 4.8.2.3 Signalling and data flow

The data flow of this procedure is depicted in Figure 4-39. Three initial frames are used for signalling and configuring the initialisation of the procedure. Then, a predefined number of frames are allocated to the UL pilots, while the RISs cycle over their sensing configurations. A time guard is needed to allow for phase-shift switching onto each metasurface, however such time is assumed to be negligible and it is incorporated within each single frame duration. Local position estimations are performed by each RIS and the estimated data are sent to the central RISO within a frame, which next performs the final estimation.

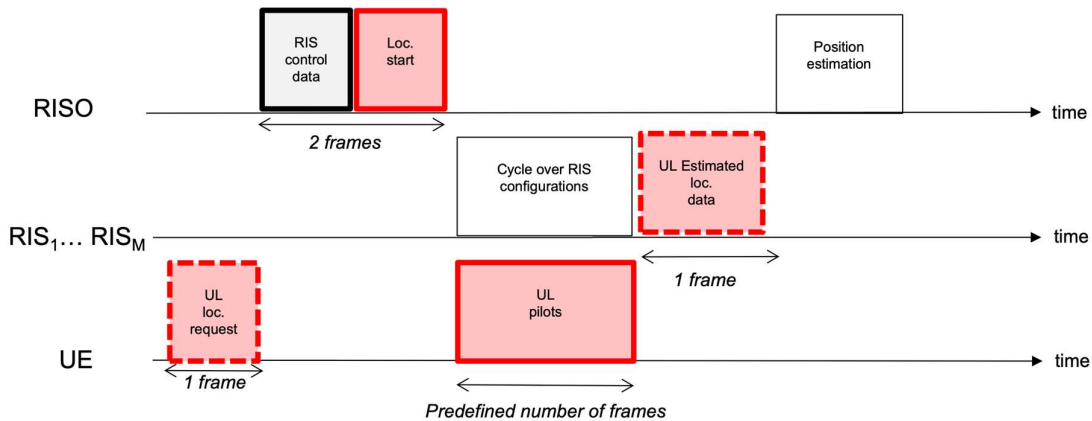


Figure 4-39: C7 - Time diagram.

#### 4.8.3 Results

The main outcomes of this work can be summarized as follows:

- Introducing a localisation scenario with multiple sensing RISs and no BSs.
- Calculating the estimation error for different number of RISs, RISs placements, and RIS configurations.
- Deriving the CRLB for the positioning and comparing with the position estimation error.



#### 4.8.4 Perspectives

This section introduced a new sensing-RIS-enabled localisation scenario, which can work in cases with no nearby BS or access points. It can also act in parallel and support transmissions or channel estimation.

### 4.9 BS-free UE localisation with one partially-connected sensing RIS (C8)

#### 4.9.1 Context and motivations

In general, to perform efficient localisation multiple receivers/RF chains are required. Usually, those RF chains are supposed to be located at different parts of the network (i.e., multiple RISs and the BS). However, a single, standalone receiving RIS with multiple partially connected RF chains may represent an alternative to that purpose.

This work is a new contribution (i.e., not reported in D5.1), which is subject to one publication [HFV+23].

#### 4.9.2 Overall system description

##### 4.9.2.1 Deployment scenario and physical architecture requirements

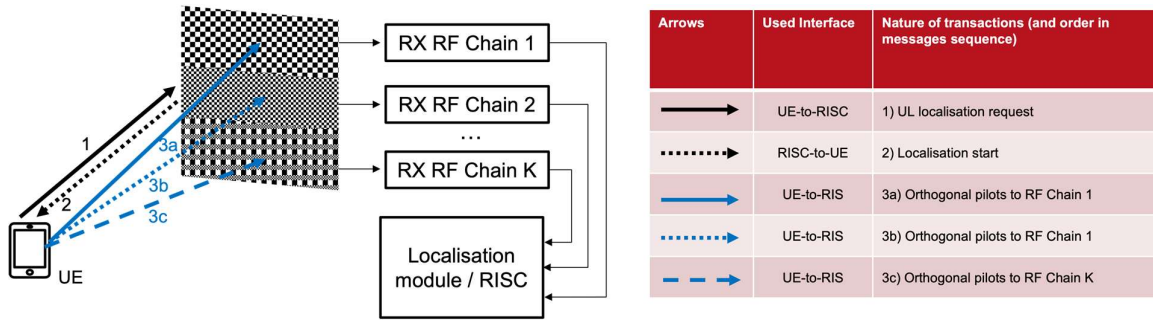


Figure 4-40: C8 - Physical deployment vs. architecture requirements, in terms of control signalling and data.

In this scenario, the RIS is comprised of  $K$  different blocks of elements. The unit-cells within a block are connected to a single RF chain, as shown in Figure 4-40. To perform localisation, the UE can send orthogonal reference signals that are received by each RF chain, converted to baseband, and then collected to the co-located localisation module that performs the localisation estimation.

##### 4.9.2.2 Control

This process requires minimal control, since, after the initial control sequences are exchanged, the RIS acts autonomously.

#### 4.9.2.3 Signalling and data flow

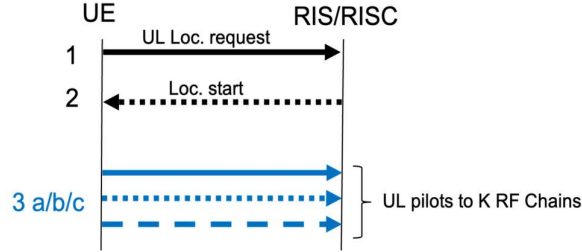


Figure 4-41 C8 - Messages sequence chart.

The messages sequence is detailed in Figure 4-41, while the corresponding timeline is shown in Figure 4-42. The UE initiates the procedure with a request, and the RIS replies with the start of the localisation procedure control message. Then the orthogonal pilots are up-transmitted while the RIS cycles through pre-defined configurations for the next number of frames (Figure 4-42), after which, the position estimation takes place.

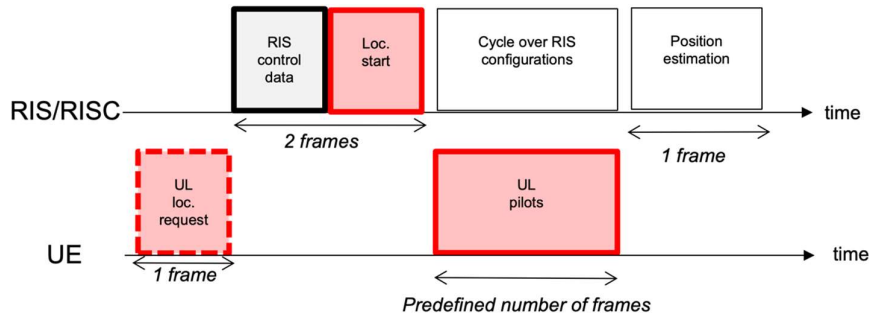


Figure 4-42: C8 - Time diagram.

#### 4.9.3 Results

Using the proposed architecture, different algorithmic schemes may be devised. In [HFV+23], the Atomic Norm Minimisation (ANM) in conjunction with subspace-based root Multiple Signal Classification (MUSIC) are proposed to extract the AoAs of the LoS channel path at each RIS subarray. This methodology is compared against the Orthogonal Matching Pursuit (OMP) estimation algorithm. The achieved Root Mean Square Error (RMSE) values over transmit power for the above schemes as well as the theoretical bound with different numbers of RF chains are shown in Figure 4-43, illustrating that the proposed scheme can achieve cm-level and beyond localisation accuracy estimates.

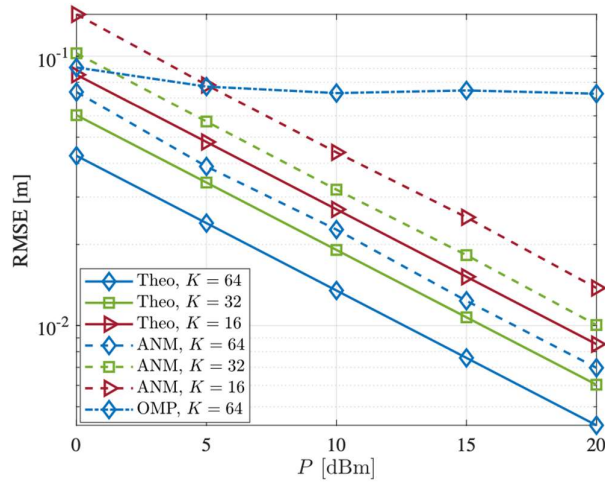


Figure 4-43: RMSE as a function of transmit power, for the architecture proposal of C8.

#### 4.9.4 Perspectives

This contribution entails a minimal network setup, as only a single RIS is required. Its main distinction with respect to contribution C3 is that this deployment strategy considers a receiving RIS instead of relying on reflected signals.

### 4.10 Single-BS NLoS UE localisation with several reflective RISs (C9)

#### 4.10.1 Context and motivations

One of the major deployment scenario of RISs is to combat blockages between the UEs and the BS by offering a reconfigurable propagation path. In the majority of cases, passive (reflecting) RISs will be deployed, therefore, the scenario of how a user may be localised when only (multiple) passive RISs are present and without direct access to the BS calls for investigation. To that end, this contribution considers such a deployment scenario and provides an analysis of the signalling and data blocks required.

This work is a new contribution (i.e., not reported in D5.1), which is subject to one publication [HFW+23].

#### 4.10.2 Overall system description

##### 4.10.2.1 Deployment scenario and physical architecture requirements

The envisioned system includes a UE with blocked access to its serving BS.  $M$  receiving RISs have been deployed in order to offer propagation paths, as shown in Figure 4-44.

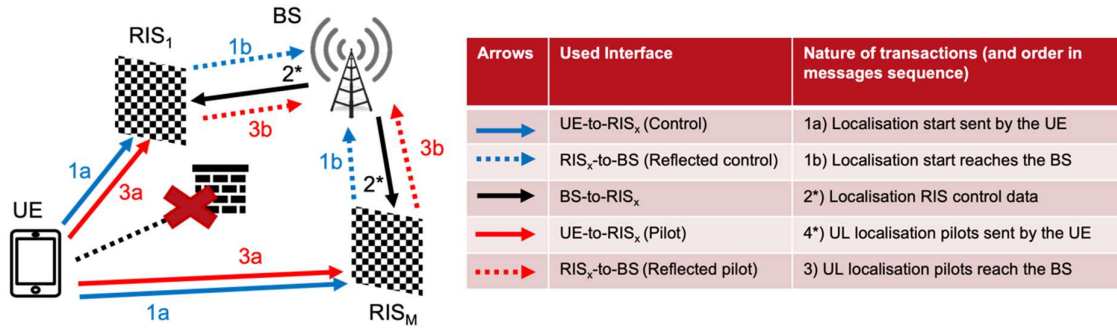


Figure 4-44: C9 - Physical deployment vs. architecture requirements, in terms of control signalling and data (\* means that data is transmitted on the over-the-air interface).

#### 4.10.2.2 Control

The BS plays the role of the centralised RIS controller, who can notify the surfaces about the start of the procedure and dictate their signalling configurations to reflect incident pilots. During the localisation process the RISs will cycle through their configurations. As it is typical with such systems, the BS needs only to notify them about the start and the parameters of the procedure, so that the internal RIS actuator selects each individual configuration autonomously. Thus, only one control message between the BS/RISC and the RISs is required. In this contribution, that message is assumed to be broadcasted (in-band or out-of-band) via the over-the-air interface between the BS and the RISs, although any type of connection can be supported.

#### 4.10.2.3 Signalling and data flow

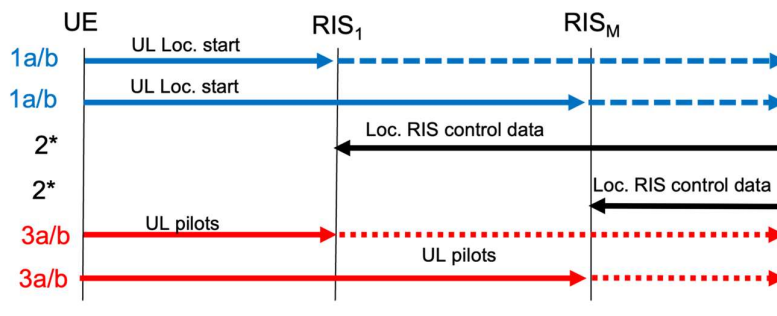


Figure 4-45: C9 - Messages sequence chart.





Document:	H2020-ICT-52/RISE-6G/D5.3		
Date:	30/06/2023	Security:	Public
Status:		Version:	1.0

The localisation procedure involves the following steps, as illustrated with the messages sequence chart in Figure 4-45 and the corresponding time diagram in Figure 4-46:

1. The UE initiates the localisation procedure by sending a “Localisation start” signal toward the RISs, which reaches the BS via reflections. In typical localisation procedures, the BS would respond with an acknowledgement (ACK) message so that the various components are synchronised. Due to the impeded communication scenario, all relevant information is assumed to be contained inside the UL control message.
2. Upon receiving the start message, the BS sends a control message to the RISs to notify them that they should start cycling through their receiving configurations.
3. The UL reference signal transmissions then start. The pilots are collected by the BS via the RIS reflections. This procedure takes a predefined number of frames. The RISs switch configurations after each pilot packet is received to facilitate the algorithmic estimation phase.

In this case, the RISC, which is likely situated together with the BS, performs the algorithmic estimation and attains the 3D position of the UE.

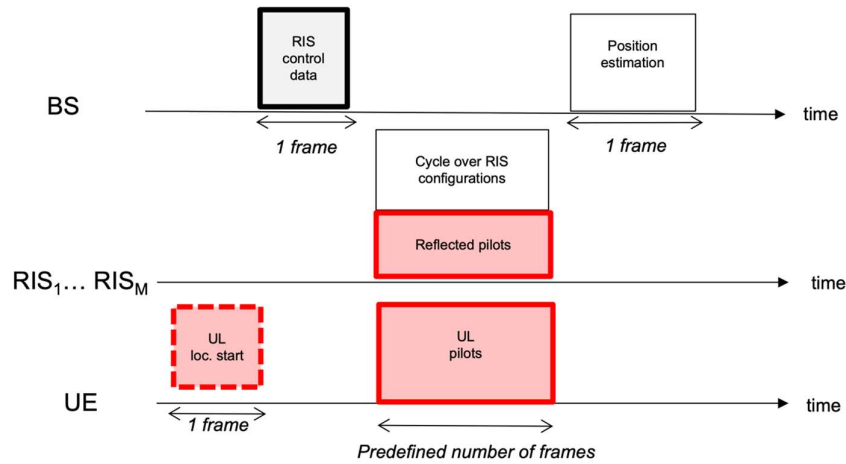


Figure 4-46: C9 - Time diagram.

#### 4.10.3 Results

In the accompanying publication, the sparsity of information appearing in the multiple reference signals and cycled configurations is exploited via compressed sensing algorithms [HFW+23]. The duration of the reference signals along with the needed size of the RIS are considered. To allow for informative comparison, the CRLB has been derived. The numerical results displayed in the following Figure 4-47 and Figure 4-48 illustrate that, for the deployment of 3 to 4 RISs and the use of 32 training pilots, 64 to 100 elements per RIS are enough to achieve results that approach the theoretical CRLB limit.

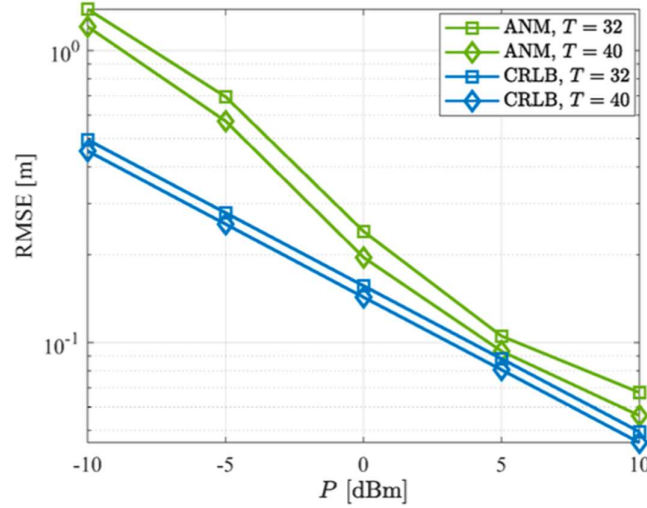


Figure 4-47: Position estimation RMSE of proposed approach of C9 (ANM) over transmit power  $P$ , compared to the theoretical CRLB.  $T$  means the number of pilot packets required.

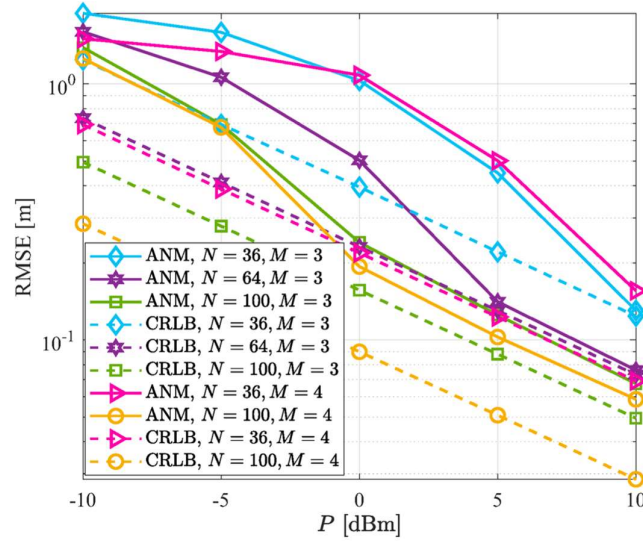


Figure 4-48: The effect of the number of BS antennas  $N$  and that of RISs  $M$  on the performance of the proposed 3D localisation system (ANM) and the theoretical CRLB over transmit power  $P$ .

#### 4.10.4 Perspectives

This methodology provides an effective solution when passive RISs are deployed to combat BS-UE blockages. While other contributions provide more elaborate systems with localisation via multiple RISs, even without the need for a BS, the important difference is that this contribution assumes simple reflecting metasurfaces.

## 4.11 Localisation of both active and passive UEs with one sensing RIS (C10)

### 4.11.1 Context and motivations

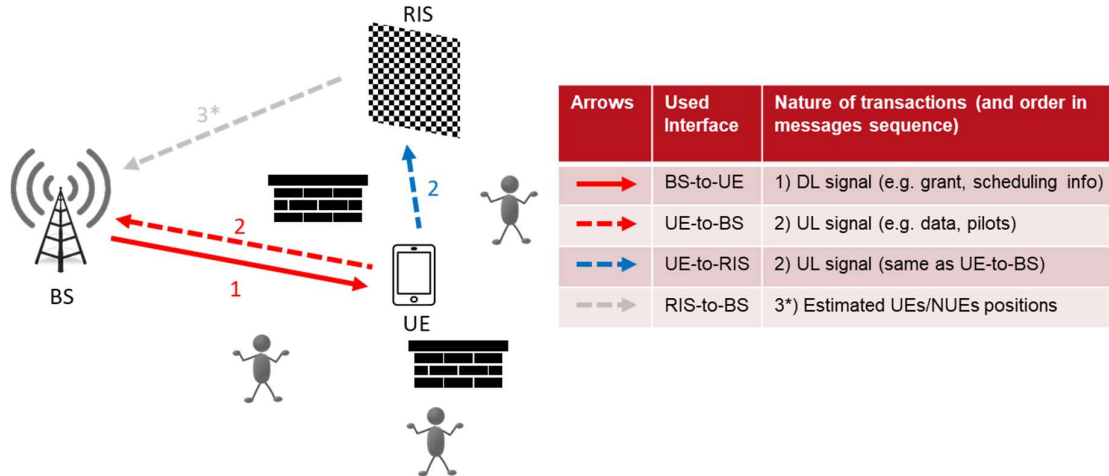
Motivated by their future integration in communication systems, in this work, we are focusing on the sensing capabilities of RIS and investigate their potential to detect passive users. Such functionality can be important in human intrusion detection. It also allows to optimize beam-forming towards the passive devices already during their initial access phase. We rely on the arbitrary wireless signals occurring in the environment and we process them directly from the RIS viewpoint to obtain a radio map, which describes the physical presence of passive devices. We make use of machine learning, image processing and computer vision techniques to extract meaningful information from these radio maps. Finally, we evaluate the proposed method for both active and passive user detection in an indoor setting.

This work is an extension of the initial contribution reported in D5.1 [Sec. 4.3.4, RIS5.1-22], which is subject to one publication [VRK+22].

### 4.11.2 Overall system description

#### 4.11.2.1 Deployment scenario and physical architecture requirements

The system comprises a BS or access point (AP), a sensing RIS,  $U_a$  active (transmitting) users and  $U_p$  passive non-intended users (NUEs). Example is shown in Figure 4-49. The system is not limited to cellular technologies, as it can use other wireless signals (such as WiFi) to carry out sensing.



**Figure 4-49: C10 - Physical deployment vs. architecture requirements of [VRK+22], in terms of control signalling and data (\* means that data is transmitted on the over-the-air interface).**

#### 4.11.2.2 Control

The control procedures in this scheme are purposely kept to the minimum. As mentioned earlier, the system does not rely on signals specific to the cellular technologies; in particular, there is no need for dedicated control channels. The sensing is carried out based on the arbitrary uplink signals transmitted by active UE(s) as a part of their communication with the BS/AP. The received signal (after being subject to scattering from passive elements and users) is processed locally at the RIS to determine the positions of the objects. There is an optional RIS-to-BS link, in case the position information estimated by the RIS needs to be forwarded to the BS.

#### 4.11.2.3 Signalling and data flow

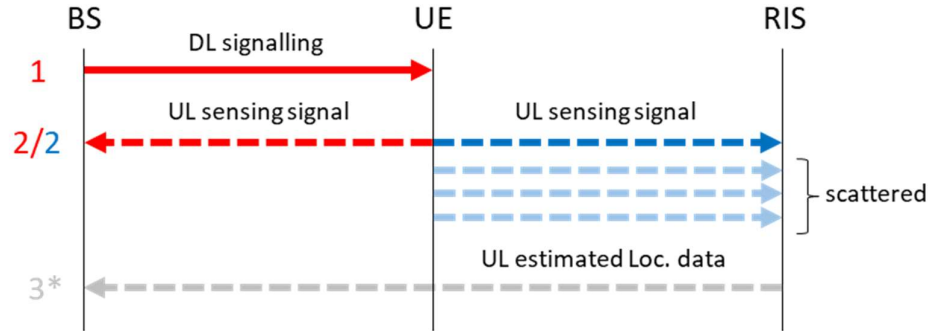


Figure 4-50: C10 - Messages sequence chart.

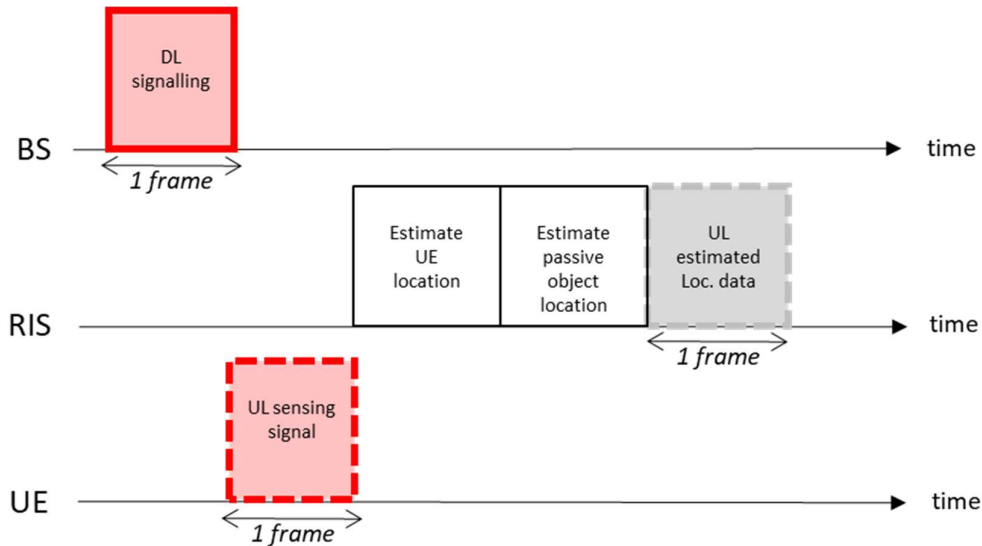


Figure 4-51: C10 - Time diagram.

The procedure involves the following steps, as illustrated in Figure 4-49 to Figure 4-51.

1. While the localisation is based on the arbitrary uplink signals transmitted by active UE, the communication is typically initiated by the BS (or Access Point (AP)). This preceding DL signal could be the access grant, scheduling information or explicit "localisation start" instruction sent to the UE.
2. Upon receiving the relevant signal from the BS/AP, the UE starts transmitting its own uplink signal in response. The transmission could concern simply the payload, pilots or a dedicated sensing signal.
3. The UL signal transmitted by the UE is received by the sensing (hybrid) RIS (after being subject to scattering from passive elements and users). This signal is processed locally at the RIS to
  - a. Estimate the position of the active (transmitting) UEs
  - b. Create a negative mask based on the positions of active UEs and fixed scatterers

- c. Apply the negative mask to the received signal to determine the positions of the remaining passive (not-transmitting) users
4. (optional) RIS may forward the estimated active and passive UE positions to the BS/AP for further processing.

#### 4.11.3 Results

Figure 4-52 shows the localisation outcome of the proposed technique in an example scenario with 10 passive humans in the room. Figure 4-53 shows the average passive (human) detection for different amount of active random devices in the area. The results show that the higher the number of active transmitters, the more passive humans can be detected using the proposed method; nevertheless, even with very few transmitters, a detection of at least 80% of the people in the scenario is achievable. The average positioning error is around 28 cm.

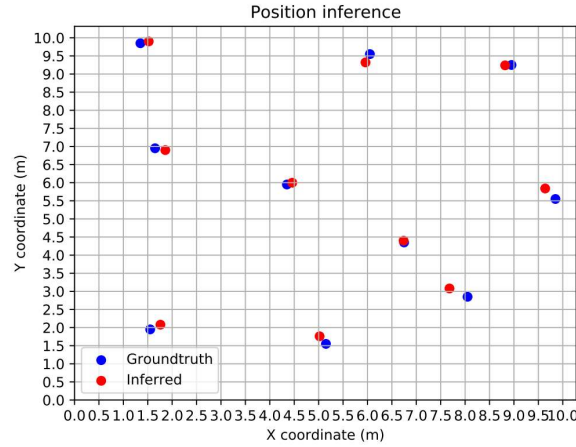


Figure 4-52: Exemplary human detection with fixed RIS aperture of  $M = 259 \times 259$ , in a  $\gamma = 0$  dB condition, with  $S = 100$  averaging strategy,  $U_a = 20$  active users and  $U_p = 10$  passive users in the scenario.



Figure 4-53: Average human detection percentage (%) and positioning errors (cm) with fixed RIS aperture of  $M = 259 \times 259$ , in a  $\gamma = 0$  dB condition, with  $S = 100$  averaging strategy and  $U_p = 10$  passive users in the scenario for different numbers of active devices  $U_a$ .



Document:	H2020-ICT-52/RISE-6G/D5.3		
Date:	30/06/2023	Security:	Public
Status:		Version:	1.0

#### 4.11.4 Perspectives

The proposed technique focuses on the use cases with sensing RIS capable of local processing. As such, it requires no (or very little) signalling between the BS and RIS, which might be attractive in some deployment scenarios. The ability to detect active and passive UEs is crucial for the electromagnetic field (EMF) avoidance and management techniques investigated in WP6.

## 5 Candidate architectures and control schemes for physical laboratory demonstrations and field trials of RIS-aided localisation and sensing

In this section, we describe concrete experimental setups and scenarios considered in WP7 for both the laboratory validation and/or the field trial demonstration of WP5 localization and sensing proposals, mostly from an architecture and control standpoint, while algorithmic aspects related to these validations will be addressed in upcoming deliverable D5.4. As for the final results of these experimental validations, they will be accounted in the final D7.3 deliverable.

### 5.1 Offline laboratory experiments

#### 5.1.1 Experimental validation of single-BS localization and mapping at 28 GHz

These first experiments are intended primarily to demonstrate the capability of reflective RISs to enable:

- Localization in simple scenarios for which conventional systems would fail (due to missing links/measurements and/or to poorly informative radio metrics), putting emphasis mostly on deployment (and hence, architecture) aspects, rather than on control or estimation algorithms. Accordingly, basic channel estimation algorithms (e.g., high-resolution Space-Alternating Generalized Expectation-maximization (SAGE)) and simple directional RIS beams are considered. The capability to locally boost positioning performance is also tested by sequentially using RIS reflections on top of a direct path.
- Simultaneous localization and mapping (SLAM) based on the same radio metrics, while relying on different measurement snapshots (wrt. to both BS and RIS beams scanning).

These validations are related to the physical architecture and simplest directional RIS control strategy described in Contribution C1 (see Section 4.2).

##### 5.1.1.1 Hardware equipment and main system specifications

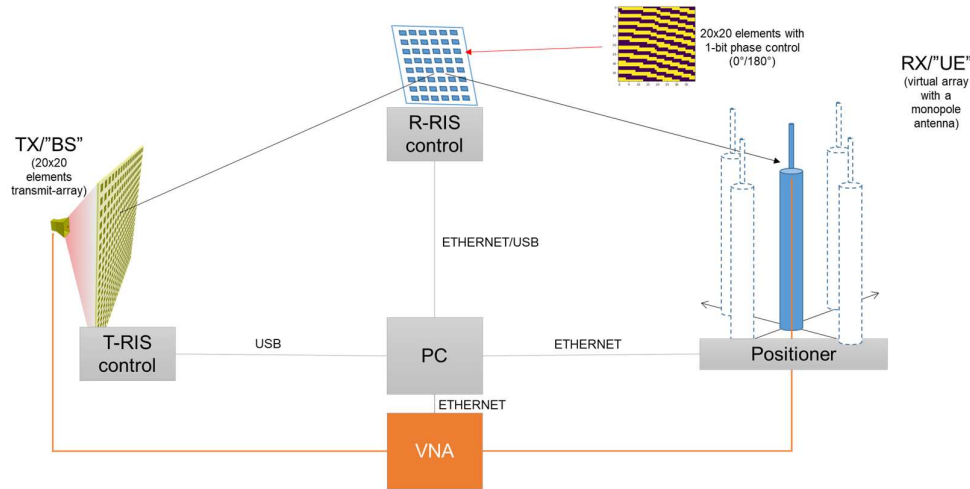
The setup used for this first mmWave experimental validation campaign relies on a Vector Network Analyser (VNA) based channel sounder used in [MdEO22], except the addition of both a T-RIS on the transmitter (TX) side and a Reflective RIS (R-RIS) between the TX and the receiver (RX), which was designed by Greenerwave in WP3 [RIS3.2-22]. Note that by the time this report is written, a second measurement campaign is scheduled based on another RRIS prototype designed by CEA also in the frame of WP3.

Figure 5-1 shows a simplified block diagram of the overall measurement acquisition chain, which is composed of:

- T-RIS and R-RIS both composed of 20x20 elements with 1-bit phase control, operating around 28 GHz and with possibility to select the point beam direction from  $-60^\circ$  to  $+60^\circ$ , by the same step of  $5^\circ$ ,

- VNA recording the overall frequency-domain complex channel response between the TX and the RX, from 25 to 35 GHz,
- Monopole antenna (on UE side) with 3x3 positioner to optionally create a virtual array.

Table 5-1 details the main characteristics of the used R-RIS, as core building block of this demonstration.



**Figure 5-1: Simplified block diagram of the RIS-enabled mmWave VNA-based channel sounder, with 1-bit R-RIS phase control, used for offline validations of RIS-enabled single-BS localisation feasibility.**

Parameter	Value
Dimension	350 mm * 260 mm * 40 mm
Nb of elements	Up to 4 tiles of 20 x 20 each
Weight (RIS only)	1.8 kg
Interface	micro USB
Frequency range of operation	26.0-30GHz
Polarization	H-pol and V-pol
Scan Range (Azimuth, Elevation)	+/- 60°
3dB-beamwidth at boresight direction	tunable from 3° to 9°
RF power dissipation at reflection, max	<2dB
Beam Steering rate	<50 ms
RF Power Handling	max 50W
Average Power Consumption average 1 polarization / 2 polarizations	10W / 22W
Power Consumption max / min	42W / 6W
Control software	Python 3.8.5

**Table 5-1: Main characteristics of the R-RIS used for demonstrating RIS-enabled single-BS localisation.**



The equivalent localization system emulated offline through these experiments can thus be summarized as follows:

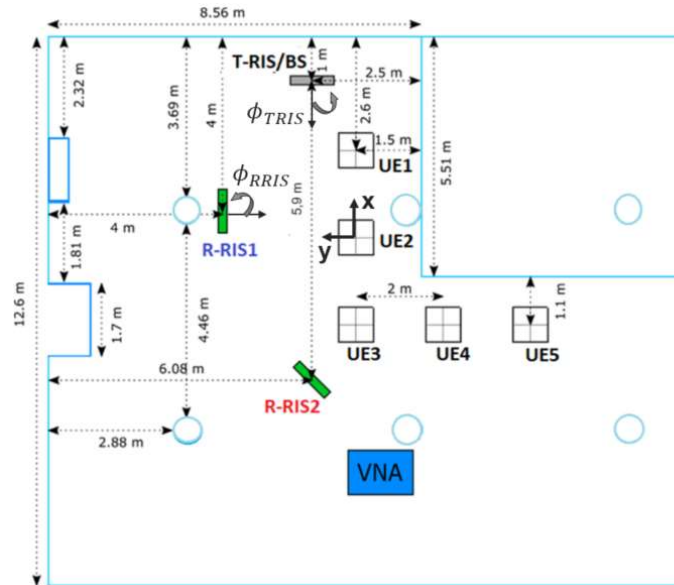
- 1 TX BS
- 1 to 2 R-RIS with directional beams (controllable through code books)
- 1 RX UE with
  - 3x3 antenna → Complex received samples, enabling multipath channel estimation (delay, AoA...) *or*
  - Single-antenna → Received Signal Strength (RSS) only (equivalently, overall channel gain with VNA measurements in our experiments)

For this setting, AoDs at both the BS and the RIS(s) can also be determined based on the measured RSSs (or the estimated multipath components (MPC) gains) at the UE, assuming that a beam scanning is performed in azimuth.

Furthermore, as we operate with a VNA in the acquisition chain, TX-RX synchronization is inherently solved and any estimated delay directly coincides with the absolute time of flight, after calibration. In a real asynchronous system relying on relative delay estimation at the RX, either multi-way protocol exchanges or joint localization and synchronization algorithms would be necessary.

#### 5.1.1.2 Foreseen scenarios

Both the floor plan of the reference indoor environment and the tested deployment configurations are represented in Figure 5-2.



**Figure 5-2: Layout and deployment information of the reference indoor environment considered for the mmWave channel measurement campaign and the related RIS-aided positioning experiments, incl. 1 BS location, 2 R-RIS locations (R-RIS 1 and 2) and 5 UE locations (UE1 to UE5).**

First, the emulated BS on the TX side (i.e., the T-RIS), which was lying in one single reference location for all the tested configurations, performed a scanning of this environment in azimuth, while the R-RIS was still off. For each beam pointing direction, a frequency-domain complex channel response was recorded between the TX and the RX. Then, using a static beam, the T-RIS just illuminated the activated R-



Document:	H2020-ICT-52/RISE-6G/D5.3		
Date:	30/06/2023	Security:	Public
Status:		Version:	1.0

RIS, which was tested sequentially within two distinct location/orientation configurations. For each location/orientation, the R-RIS was then controlled through a codebook to scan the environment in azimuth. For the scanning process of both BS and R-RIS, a unique anticlockwise convention was used to define the AoDs, a reference angle (i.e.,  $0^\circ$ ) normal to the surface/array. For each of the tested measurement configurations above, the full measurement procedure was repeated for 5 main UE positions. In each position, the RX monopole antenna was moved over the  $3 \times 3$  small-scale grid (i.e., considering a virtual  $3 \times 3$  array in the horizontal  $x$ - $y$  plane) thanks to a high-precision positioner, and a complex channel response was recorded over the same frequency band. Note that the three involved entities (i.e., BS, R-RIS and UE) were all set at the same height and hence, lying on the same 2D plane. At the end of the day, a total of 3375 complex channel responses could hence be recorded.

In all the foreseen positioning configurations tested in these first experiments, both the positions and the orientations of the BS and/or the R-RIS are assumed to be perfectly known. The following table summarizes the corresponding scenarios, depending on the combination of location-dependent radio features extracted from the channel responses. From a protocol standpoint in a real system, the scenarios making use of several MPCs (i.e., all except 0, 2d and 2e) would necessitate a sequential illumination sequence from the BS (e.g., BS first, and then RISs), coming up with one set of estimated location-dependent radio parameters for each pointing direction, which need to be recombined offline for positioning.

Scenario	MPCs [Nb R-RISs]	LoS/NLoS Status	Radio Metrics [Method]	Expected RIS Benefits
0	DP only [0 R-RIS]	LoS	DP AoD and Delay [SAGE MPCs]	N/A (Baseline)
1a	DP + RP1 [1 R-RIS]	LoS	DP AoD, RP1 AoD [Overall Channel Gain]	Enabled localization <sup>*</sup>
1b	DP + RP2 [1 R-RIS]	LoS	DP AoD, RP2 AoD [Overall Channel Gain]	Enabled localization <sup>*</sup>
1c	DP + RP1 + RP2 [2 R-RISs]	LoS	DP AoD, RP1 AoD, RP2 AoD [Overall Channel Gain]	Enabled localization <sup>*</sup>
1d	RP1 + RP2 [2 R-RISs]	NLoS	RP1 AoD, RP2 AoD [Overall Channel Gain]	Enabled localization <sup>*</sup>
2a	DP + RP1 [1 R-RIS]	LoS	DP AoD and Delay, RP1 AoD and Delay [SAGE MPCs]	Boosted localization <sup>**</sup>
2b	DP + RP2 [1 R-RIS]	LoS	DP AoD and Delay, RP2 AoD and Delay [SAGE MPCs]	Boosted localization <sup>**</sup>
2c	DP + RP1 + RP2 [2 R-RISs]	LoS	DP AoD and Delay, RP1 AoD and Delay, RP2 AoD and Delay [SAGE MPCs]	Boosted localization <sup>**</sup>
2d	RP1 [1 R-RIS]	NLoS	RP1 AoD and Delay [SAGE MPCs]	Enabled localization <sup>***</sup>
2e	RP2 [1 R-RIS]	NLoS	RP2 AoD and Delay [SAGE MPCs]	Enabled localization <sup>***</sup>
2f	RP1 + RP2 [2 R-RISs]	NLoS	RP1 AoD and Delay, RP2 AoD and Delay [SAGE MPCs]	Enabled localization <sup>***</sup>

**Table 5-2: Tested positioning scenarios (DP: Direct path, RP: RISx-reflected path on R-RISx); Expected RIS benefits: \* vs. conventional single-BS positioning using also RSS measurements, \*\* vs. conventional single-BS positioning with similar MPCs estimation capabilities but relying on DP only, \*\*\* vs. conventional single-BS positioning with similar MPCs capabilities, but relying on DP only or with no extra SLAM capabilities.**

As for SLAM validations, we will leverage exactly the same measurement configurations and metrics as that used in the basic positioning scenarios described above, all except but the fact that we will make use of several acquisition snapshots though for being able to issue a SLAM estimation result.

### 5.1.2 Experimental validation of RIS-aided self-localization at 60 GHz

The purpose of this demonstration is to show the feasibility of localizing a full-duplex UE without any BSs / access points, with the aid of only a reflective RIS. The RIS cycles through a set of directional configurations, while the UE measures the time-of-arrival (and thus the distance) for each configuration. The configuration with the largest receive power determines the AoD from the RIS, which combined with the ToA allows the UE to localize itself in the frame of reference of the RIS (i.e., performing relative positioning).

These validations are related to the physical architecture and RIS control strategy proposed in Contribution C3 above (see Section 4.4).

#### 5.1.2.1 Hardware equipment and main system specifications

The equivalent localization system emulated offline through these experiments can be summarized as follows:

- 1 full-duplex UE emits Frequency Modulated Continuous Wave (FMCW) signals at 60 GHz with 120° azimuth and 30° element field-of-views, equipped with FMCW radar consisting of four Rx and three Tx antennas,
- 1 active R-RIS generates directional beams (controllable through code books) in the azimuth plane by redirecting the radar signal from  $-45^\circ$  to  $45^\circ$  with a  $1.5^\circ$  step size.
- The UE captures baseband IQ samples for range-Doppler processing for each beam by mixing the reference transmitted waveform and the received FMCW signals reflected by objects, digitized with a low-rate Analog to Digital Converter (ADC) and applying Fast Fourier Transform (FFT) on the data samples, as shown in Figure 5-3. In the range-Doppler plot, the RIS should be visible as a distinct object.

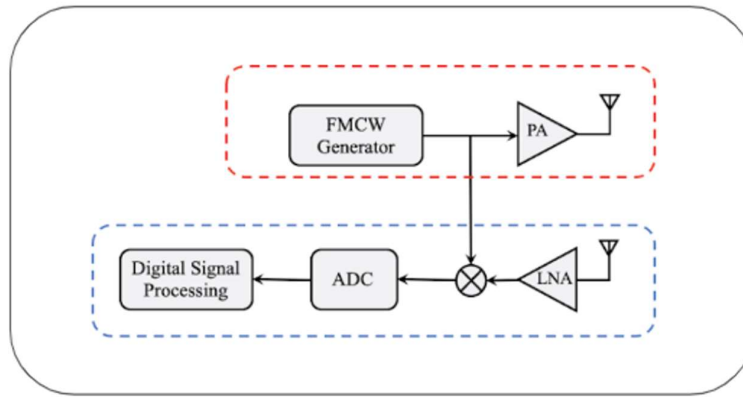


Figure 5-3: Analog and digital components of the FMCW radar at the UE

#### 5.1.2.2 Foreseen scenario

Figure 5-4 shows the testbed environment and hardware components for the FMCW radar-RIS pair. For collecting data in a real-world measurement scenario, off-the-shelf components are adopted. We utilize AWR6843ISK MIMO radar from Texas Instrument as the FMCW radar and EVK06002 from Silvers Semiconductors as the RIS. The FMCW radar transmits chirp signals propagated in the testbed environment, where the RIS redirects the received signals from  $-45^\circ$  to  $45^\circ$  with a  $1.5^\circ$  step size. Then, the FMCW radar receives the back-propagated signals and estimates range, angle, and Doppler.

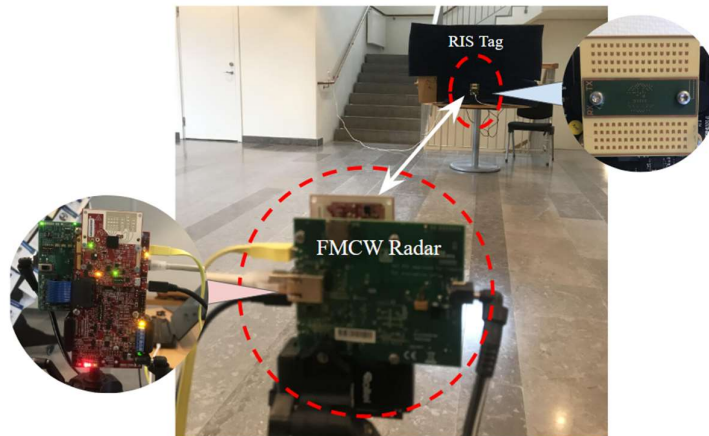


Figure 5-4: Demonstration of the testbed and components for the FMCW radar-RIS pair.



---

Document:	H2020-ICT-52/RISE-6G/D5.3		
Date:	30/06/2023	Security:	Public
Status:		Version:	1.0

---

### 5.1.3 RIS-aided fingerprinting positioning at 3.7 GHz

The purpose of this demonstration is to show the feasibility of localizing a UE with the aid of a RIS and a BS, even in a cluttered environment at low carrier frequencies. The approach is based on supervised learning, where in each training location RSS fingerprints are collected for each RIS configuration. These fingerprints represent a smooth function of the underlying location. This smooth relation can be used to determine the location of a UE based on the fingerprint.

These validations are related to some extent to the physical architecture and RIS control proposals C10 above (see Section 4.11).

#### 5.1.3.1 Hardware equipment and main system specifications

The equivalent localization system emulated offline through these experiments can be summarized as follows:

- 1 commercial Nokia 5G Non-Standalone (NSA) BS operating at 3.7 GHz (details can be found in D7.1), which is connected to the TIM live network by an optic fibre.
- 1 R-RIS with a predetermined set of configurations (from a codebook). The device is foreseen to be equipped with an array of 10x10 patch antennas operating at 3.7 GHz mounted on Printed Circuit Board (PCB) with fr4 150 substrate and connected to a central Microcontroller Unit (MCU). The total dimension of the device is expected to be 40x40 cm with a thickness of 1.2 mm. Each patch antenna is connected to an RF-switch that can be configured by the MCU in one of 4 states (2-bit phase-shifting capability), which are represented by delay lines of different lengths, similarly to the design proposed in [RMG+22].
- 1 commercial Askey outdoor UE (New Radio (NR) Outdoor Unit (ODU)) which supports both 4G LTE and 5G NR connectivity (NSA) compatible with 3GPP Release 15 (details can be found in D7.1). During the tests, it allows to collect Reference Signal Received Power (RSRP) data. Moreover, a smartphone via a Test Mobile System (TEMS) app (i.e., an application used by mobile operators to measure, analyse and monitoring their networks) could be used as well.

#### 5.1.3.2 Foreseen scenario

Measurements will be collected in an indoor office environment. We consider that the BS (transmitter) and the RIS are in two different fixed locations, while the UE (receiver) can assume  $L$  different positions inside a specific area. The RIS-aided wireless fingerprinting localization process is performed in two phases:

- We collect the RSSI values received by the UE to form two fingerprint databases of the position grids. The first database ( $DB1$ ) is established in a scenario without the RIS, where the transmitter (BS) and the receiver (UE) communicate through a direct link. We collect a vector of  $L$  fingerprints, corresponding to each  $l$  in  $L$  position assumed by the UE in the location grid. The second database ( $DB2$ ) is compiled in a scenario where no direct link can be established between the BS and the UE (blockage event), and we leverage a RIS-aided communication link. The BS transmits continuous pilot signals, while the RIS cycles through  $M$  different configurations. Then, for each position  $l$ , we collect the RSSI values exploring each  $m$  in  $M$  RIS's configuration, forming an  $L \times M$  fingerprints matrix.
- During the second phase, the UE is placed at an unknown position  $x$  in  $A$ . Thus, we collect a single RSSI value received from the BS (in case of  $DB1$ ) or a vector of  $M$  signal strength measurements (in case of  $DB2$ ). The localization is performed by comparing the current RSSI received in  $x$  with the values stored in the databases. In particular, we can find the most likely location  $x^*$  by minimizing the difference vector between the new measurements and the fingerprints databases.

The performance in the location estimate is measured through the root mean square error (RMSE), with the intention to show that fingerprinting localization based on  $DB2$  is better than the one based on  $DB1$ .



---

Document:	H2020-ICT-52/RISE-6G/D5.3		
Date:	30/06/2023	Security:	Public
Status:		Version:	1.0

---

## 5.2 Online field trials

### 5.2.1 RIS-aided Single-BS localization with commercial network and equipment in a factory environment at 27 GHz

The purpose of this demonstration is to show 3D UE localization based on directional beams with respect to at least 2 RIS, while relying on RSS measurements.

These validations represent the simplest variant to the system architecture and RIS control proposal in Contribution C1 above (see Section 4.2).

#### 5.2.1.1 Hardware equipment and main system specifications

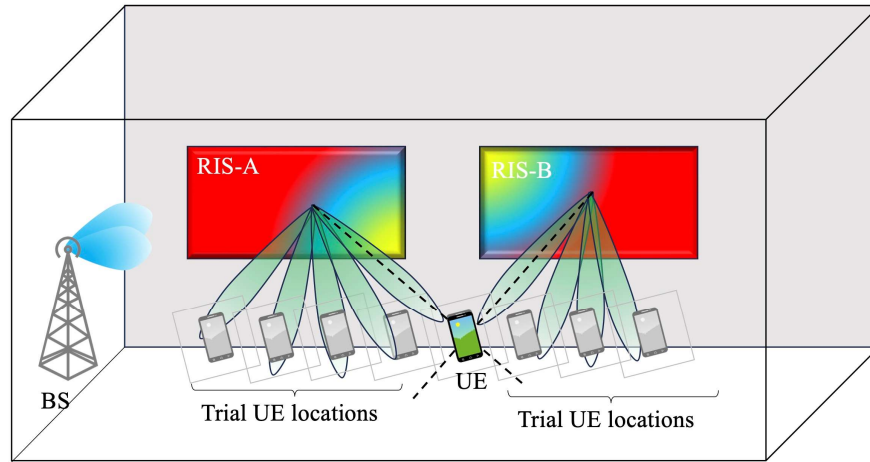
The system set-up is composed of:

- BS: a commercial Ericsson 5G NSA BS, equipped with the RF module AIR5322 operating at N258 band (licensed TIM frequency band is 26.9-27.1 GHz);
- UE terminal: a 5G CPE by ZTE, which allows to read SS-RSRP values in real-time;
- R-RIS: the RIS is that same as that already used for in-lab offline demonstration and detailed in Table 5-1, whose element phase distribution is optimized at 28 GHz.

#### 5.2.1.2 Foreseen scenario

The localization principle can be summarized as follows (see Figure 5-5):

- A BS transmits signals sequentially towards each R-RIS (first to RIS-A and later to RIS-B). The BS has location  $\mathbf{x}_{BS}$ , RIS-A has location  $\mathbf{x}_A$  and orientation  $\mathbf{R}_A$  (similarly for RIS-B). The user has location  $\mathbf{x}_{UE}$ .
- During the time the BS transmits signals towards RIS-A, RIS-A applies directional beams (say  $\mathbf{f}_1, \dots, \mathbf{f}_N$ ) towards a set of possible UE locations (say  $\mathbf{x}_1, \dots, \mathbf{x}_N$ ), according to a deterministic pattern enabling to scan the environment in azimuth. For each beam, the UE measures the received power (say,  $p_1, \dots, p_N$  for RIS-A and  $q_1, \dots, q_N$  for RIS-B). Note that the locations are defined in a global frame of reference, so that a beam towards location  $\mathbf{x}_i$  in a global frame of reference is considered to be towards  $\mathbf{R}_A^T (\mathbf{x}_i - \mathbf{x}_A)$ , in the local frame of reference of the RIS-A (similarly for RIS-B).
- For each candidate point in the set of possible UE locations, a weight is computed  $w_i = (p_i + q_i) / (\sum_j p_j + q_j)$ , based on received powers. Then, the pairs  $(w_i, \mathbf{x}_i)$  represent a probability mass function of the UE location, which somehow accounts for the probability that the UE lies in each candidate test/trial location.



**Figure 5-5: Principle of the online field trial for single-BS RIS-aided single-BS localisation within commercial network (the so-called “trial” locations correspond to the tested candidate UE locations).**

## 6 Conclusions and final recommendations

One major interest of the RISs lies in their ability to provide localisation and sensing functionalities besides communications. This is particularly relevant in scenarios where traditional network architectures prove inadequate or fall short due to missing information (i.e., limited number of links, too few measurements, or too small bandwidth, etc.). In general, RISs enable the accurate estimation of controlled multipath parameters or the acquisition of rich sets of complex signals, respectively for localising connected users or sensing passive users. However, acquiring such information requires fine RIS control capabilities, adequate signalling and data flows to support RIS activation and remote control (e.g., for BS-RIS synchronisation, exchange of prior information...), as well as a relevant partitioning of the logical functions required at architecture level. In this deliverable, ten distinct proposals have been put forward (incl. variants), regarding mostly physical architecture/deployment, signalling, and control aspects.

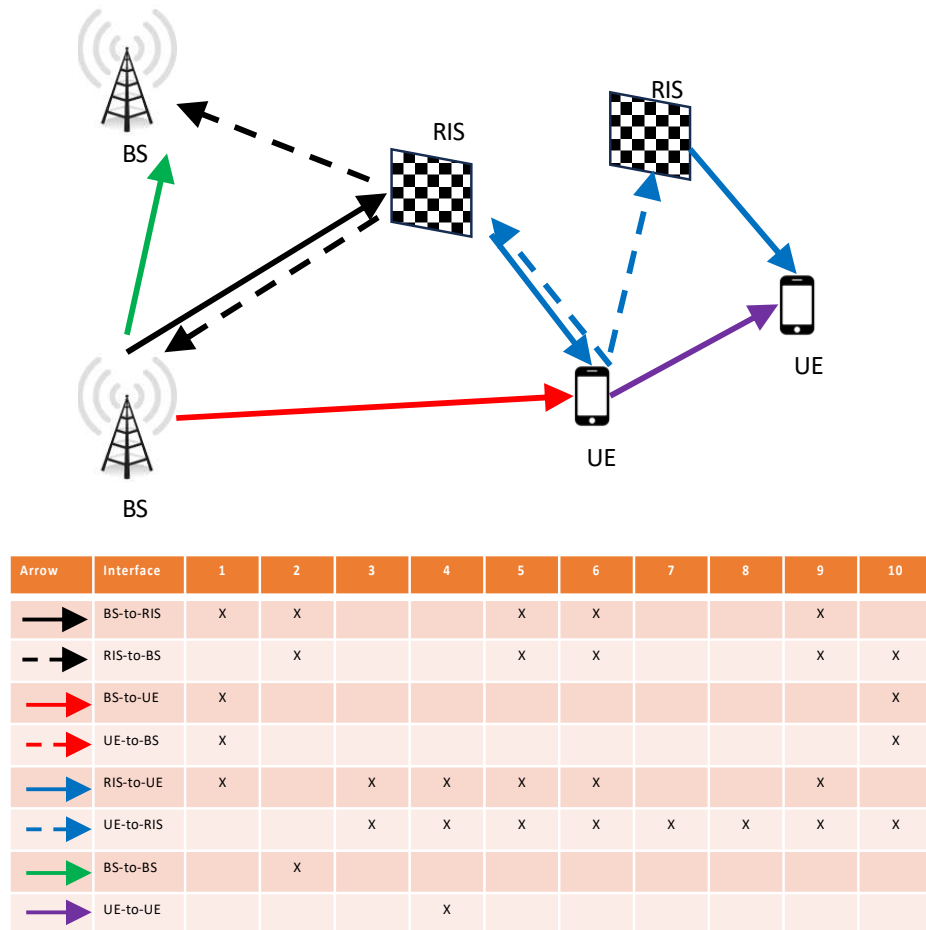
Table 6-1 and Figure 6-1 summarise the main proposals and the associated requirements in terms of control signalling for the RISE-6G architecture.

Contribution	Name	Section	Objective
1	Single-BS UE localisation with reflective RISs (C1)	4.2	UE localisation
2	Passive RIS localisation with several BSs (C2)	4.3	RIS localisation
3	BS-free UE localisation and environment mapping with one reflective RIS (C3)	4.4	UE localisation, sensing
4	BS-free cooperative UE localisation through sidelinks with one reflective RIS (C4)	4.5	UE localisation
5	Single-BS UE localisation with one reflective RIS in near field (C5)	4.6	UE localisation



6	Single-BS UE localisation with one reflective RIS in near field under real hardware constraints (C6)	4.7	UE localisation
7	BS-free UE localisation with several sensing RISs (C7)	4.8	UE localisation
8	BS-free UE localisation with one partially-connected sensing RIS (C8)	4.9	UE localisation
9	Single-BS NLoS UE localisation with several reflective RISs (C9)	4.10	UE localisation
10	Localisation of both active and passive UEs with one sensing RIS (C10)	4.11	UE localisation, sensing

**Table 6-1: Considered proposals related to RIS control for localisation and sensing**



**Figure 6-1: Physical architecture requirements in terms of control signalling for all the proposed localisation and sensing schemes.**





Document:	H2020-ICT-52/RISE-6G/D5.3		
Date:	30/06/2023	Security:	Public
Status:		Version:	1.0

The main findings of this work can be summarised as follows:

- A **multitude of physical architectures** are possible for RIS-aided localisation and sensing, not only to boost or enable positioning, but also to drastically reduce reliance on more complex and power-greedy elements of infrastructure, such as active BSs. These solutions address various operating trade-offs and applications, while coping with distinct deployment constraints. Depending on the application scenario, a RIS can be perceived either as an integral component of the infrastructure, hence requiring explicit knowledge of its spatial coordinates and angular orientation, or as an intrinsic part of a user device, necessitating the estimation of the RIS's positioning and orientation.
- The **selection of the RIS profiles** (typically, phase profiles) strongly impacts positioning accuracy. These profiles span from random (in the absence of any prior information) over directional (constraining the RIS directions towards the user or a specific region) to optimal (combining directional with derivative beams for fine tracking). Localisation must also cope with inter-RIS interference, which can be achieved through orthogonalisation of the sequence of RIS profiles (i.e., in time or code space).
- In terms of **logical RIS control**, high-level tasks should be split into more elementary tasks, which are performed by the RIS controller, while the most elementary operations (i.e., with the finest time granularity) are carried out at the RIS itself through its RIS actuator (e.g., loading of the requested RIS configuration).
- In terms of **signalling overhead**, the level of autonomy of the individual RISC plays an important role. A RISC with significant computational and storage capabilities could locally determine optimised RIS configurations or store mappings from user location to several codebooks. A low-complexity RISC is limited by a smaller set of configurations, a subset of which must be selected externally (e.g., by the RISO).
- Assuming a minimum refresh period of 100 ms, the whole localisation procedure (for delivering one positioning result) shall be completed within 10 ms (latency), with the following time constraints:
  - Localisation and sensing usually require a plurality of RIS configurations, based on pilot transmissions. They can integrate observations over time to achieve better SNR. On the other hand, since localisation is time sensitive, the duration of pilot transmissions is limited (typically, to a few tens of milliseconds). Combined, this means that the architecture should support quick varying RIS configurations (ideally at an OFDM symbol or slot level).
  - The RIS configurations need to be changed depending on the kind of applied processing. In non-coherent processing, the overall latency budget represents the main limitation (typically,  $\sim$  every 250  $\mu$ s in non-coherent processing for 2 RIS using 20 beams each, given an overall latency budget of 10 ms), while in coherent processing, the RIS update period depends mostly on the channel coherence time (e.g., 100 ms (resp. 10 ms) at 3 GHz (resp. 30GHz) for a velocity of 1 m/s).
  - In scenarios requiring more than one RIS, every 100ms, RISO must activate/trigger clusters of RISs that must all perform their tasks within 10 ms (e.g., beam scanning).

The previous analysis has been fuelling the work currently on-going in WP2, which aims at defining a unified RISE-6G architecture by the end of the project. In particular, several options regarding the partitioning of key logical functions are currently being elaborated depending on both affordable RIS complexity (in terms of embedded computation and control capabilities) and prior application requirements (in terms of mobility/latency and target accuracy), while still relying on common generic logical blocks and interfaces (i.e., covering not only localisation and sensing, but also RIS-aided communication needs).



Document:	H2020-ICT-52/RISE-6G/D5.3		
Date:	30/06/2023	Security:	Public
Status:		Version:	1.0

## 7 References<sup>1</sup>

- [AKK+21] Z. Abu-Shaban, K. Keykhosravi, M. F. Keskin, G. C. Alexandropoulos, G. Seco-Granados, and H. Wymeersch, "Near-field Localization with a Reconfigurable Intelligent Surface Acting as Lens," Proc. IEEE ICC'21, June 2021.
- [AVW22] G.C. Alexandropoulos, I. Vinieratou, and H. Wymeersch, "Localization via multiple reconfigurable intelligent surfaces equipped with single receive RF chains," IEEE Wireless Communications Letters, 2022. Pre-print Available on ArXiv: <https://arxiv.org/abs/2202.13939>
- [CKA+23] Chen, H., Kim, H., Ammous, M., Seco-Granados, G., Alexandropoulos, G.C., Valaee, S. and Wymeersch, H., 2023. RISs and Sidelink Communications in Smart Cities: The Key to Seamless Localization and Sensing. *arXiv preprint arXiv:2301.03535*.
- [DZD+20] M. Di Renzo, A. Zappone, M. Debbah, M. S. Alouini, C. Yuen, J. De Rosny, & S. Tretyakov, "Smart radio environments empowered by reconfigurable intelligent surfaces: How it works, state of research, and the road ahead." IEEE Journal on Selected Areas in Communications 38.11 (2020): 2450-2525.
- [GD21] F. Guidi and D. Dardari, "Radio Positioning with EM Processing of the Spherical Wavefront," in IEEE Transactions on Wireless Communications, vol. 20, no. 6, pp. 3571-3586, June 2021.
- [GKC+22] R. Ghazalian, K. Keykhosravi, H. Chen, H. Wymeersch, R. Jäntti, "Bi-Static Sensing for Near-Field RIS Localization," in Proc. IEEE GLOBECOM, Rio de Janeiro, Brazil, Dec. 2022.
- [HFW+23] J. He, A. Fakhreddine, H. Wymeersch, and G. C. Alexandropoulos, "Compressed-sensing-based 3D localization with distributed passive reconfigurable intelligent surfaces," IEEE International Conference on Acoustics, Speech, and Signal Processing, Rhodes, Greece, 4–9 June 2023, to be presented.
- [HFV+23] J. He, A. Fakhreddine, C. Vanwysberghe, H. Wymeersch, and G. C. Alexandropoulos, "3D localization with a single partially-connected receiving RIS: Positioning error analysis and algorithmic design," IEEE Transactions on Vehicular Technology, under revision, 2023.
- [KCK+22] Kim, H., Chen, H., Keskin, M.F., Ge, Y., Keykhosravi, K., Alexandropoulos, G.C., Kim, S. and Wymeersch, H., 2022. RIS-enabled and access-point-free simultaneous radio localization and mapping. *arXiv preprint arXiv:2212.07141*.
- [KDA+23] Keykhosravi, K., Denis, B., Alexandropoulos, G.C., He, Z.S., Albanese, A., Sciancalepore, V. and Wymeersch, H., 2023. Leveraging Ris-Enabled Smart Signal Propagation for Solving Infeasible Localization Problems: Scenarios, Key Research Directions, and Open Challenges. *IEEE Vehicular Technology Magazine*.
- [KKD+21] K. Keykhosravi, M. F. Keskin, S. Dwivedi, G. Seco-Granados, and H. Wymeersch, "Semi-passive 3D positioning of multiple RIS-enabled users", in IEEE Transactions on Vehicular Technology, vol. 70, no. 10, pp. 11073-11077, Oct. 2021. Pre-print Available on ArXiv: <https://arxiv.org/abs/2104.12113>

<sup>1</sup> Papers from the RISE-6G project related to D5.3 are provided with Arxiv.org links.



Document:	H2020-ICT-52/RISE-6G/D5.3		
Date:	30/06/2023	Security:	Public
Status:		Version:	1.0

- [KKS+21b] K. Keykhosravi, M. F. Keskin, G. Seco-Granados, and H. Wymeersch, “SISO RIS-enabled joint 3D downlink localization and synchronization,” in Proc. IEEE International Conference on Communications, June 2021. Pre-print available on ArXiv: <https://arxiv.org/abs/2011.02391>
- [KSA+22] K. Keykhosravi, G. Seco-Granados, G. C. Alexandropoulos, and H. Wymeersch, “RIS-Enabled Self-Localization: Leveraging Controllable Reflections with Zero Access Points”, in Proc. IEEE International Conference on Communications, Seoul, South Korea, 16–20 May 2022. Pre-print available on ArXiv: <https://arxiv.org/abs/2202.11159>
- [MdEO22] A. Mudonhi, R. D’Errico, and C. Oestges, “Analysis of multipath components distributions over a large array in indoor mmwave channels,” IEEE Trans. on Antennas and Propagation, vol. 70, no. 9, pp. 8330–8336, 2022
- [PRL+18] J. A. del Peral-Rosado, R. Raulefs, J. A. Laspez-Salcedo, and G. Seco-Granados, “Survey of cellular mobile radio localization methods: From 1G to 5G,” IEEE Commun. Surveys Tuts., vol. 20, no. 2, pp. 1124–1148, 2018.
- [RDK+21] M. Rahal, B. Denis, K. Keykhosravi, B. Uguen, H. Wymeersch, “RIS-Enabled Localization Continuity Under Near-Field Conditions”, Proc. IEEE SPAWC’21, Sept. 2021. Pre-print available on ArXiv: <https://arxiv.org/abs/2109.11965>
- [RDK+22a] M. Rahal, B. Denis, K. Keykhosravi, M.F. Keskin, B. Uguen, H. Wymeersch, “Nearfield Localization-Optimal RIS Profile Design and Practical Time Sharing”, IEEE VTC 2022 – Spring, Workshop on Localization and Sensing with Intelligent Surfaces for 6G Networks, Helsinki, June 2022. Pre-print available on ArXiv: <http://arxiv.org/abs/2203.07269>
- [RDK+22b] M. Rahal, B. Denis, K. Keykhosravi, M.F. Keskin, B. Uguen, G.C. Alexandropoulos, H. Wymeersch, “Arbitrary Beam Pattern Approximation via RISs with Measured Element Responses”, EuCNC’22 & 6G Summit’22, June 2022. Pre-print available on ArXiv: <http://arxiv.org/abs/2203.07225>
- [RDK+23] M. Rahal, B. Denis, K. Keykhosravi, M.F. Keskin, B. Uguen, G.C. Alexandropoulos, H. Wymeersch, “Performance of RIS-Aided Near\_eld Localization under Beams Approximation from Real Hardware Characterization”, EURASIP Journal on Wireless Communications and Networking (EURASIP JWCN) - Special Issue on 6G Connectivity for a Sustainable World, 2023. Pre-print available on ArXiv: <https://doi.org/10.48550/arXiv.2303.15176> <https://arxiv.org/abs/2303.15176v1>
- [RIS2.4-22] RISE-6G Deliverable D2.4, “Metrics and KPIs for RISE wireless systems analysis: final results”, Feb. 2022
- [RIS2.5-22] RISE-6G Deliverable D2.5, “RISE network architectures and deployment strategies analysis: first results”, June 2022
- [RIS3.2-22] RISE-6G Deliverable D3.2, “RIS designs, and first prototypes characterization”, July 2022
- [RIS4.1-22] RISE-6G Deliverable D4.1, “Deployment and control strategies of RIS based connectivity (Intermediary Specifications)”, April 2022.
- [RIS5.1-22] RISE-6G Deliverable D5.1, “Control for RIS-based localisation and sensing (Intermediary Specifications)”, July 2022.
- [RIS5.2-22] RISE-6G Deliverable D5.2, “Algorithms for RIS-based Localisation and Sensing (Intermediary Specifications)”, April 2022.



---

Document:	H2020-ICT-52/RISE-6G/D5.3		
Date:	30/06/2023	Security:	Public
Status:		Version:	1.0

---

- [RIS6.1-22] RISE-6G Deliverable D4.1, “Network architectures & deployment strategies with RIS for enhanced EE, EMFEU, and SSE (Intermediary Specifications)”, May 2022.
- [RMG+22] M. Rossanese, P. Mursia, A. Garcia-Saavedra, V. Sciancalepore, A. Asadi, and X. Costa-Perez, “Designing, building, and characterizing RF switch-based reconfigurable intelligent surfaces”, in Proceedings of the 16th ACM Workshop on Wireless Network Testbeds, Experimental evaluation & CHaracterization (WiNTECH '22), 2022.
- [SZL+21] Swindlehurst, A. L., Zhou, G., Liu, R., Pan, C., & Li, M. (2021). Channel Estimation with Reconfigurable Intelligent Surfaces--A General Framework. *arXiv pre-print arXiv:2110.00553*.
- [TSF+17] J. Tranter, N. D. Sidiropoulos, X. Fu, and A. Swami, “Fast unit-modulus least squares with applications in beamforming,” IEEE Transactions on Signal Processing, vol. 65, no. 11, pp. 2875–2887, 2017.
- [VRK+22] C.J. Vaca-Rubio, et al. "Radio Sensing with Large Intelligent Surface for 6G," Proc. IEEE ICASSP'23, June 2023, Pre-print Available on ArXiv: <https://arxiv.org/abs/2111.02783>
- [WHD+20] H. Wymeersch, J. He, B. Denis, A. Clemente, and M. Juntti, “Radio localization and mapping with reconfigurable intelligent surfaces: Challenges, opportunities, and research directions,” IEEE Veh. Technol. Mag., vol. 15, no. 4, pp. 52–61, Dec. 2020.
- [WLW+18] Wen, F., Liu, P., Wei, H., Zhang, Y., & Qiu, R. C. (2018). Joint azimuth, elevation, and delay estimation for 3-D indoor localization. *IEEE Transactions on Vehicular Technology*, 67(5), 4248-4261.
- [ZGL19] Zafari, F., Gkelias, A., & Leung, K. K. (2019). A survey of indoor localization systems and technologies. *IEEE Communications Surveys & Tutorials*, 21(3), 2568-2599.